

**CARBON, WATER, AND ENERGY DYNAMICS OF A TEMPERATE  
PINE FOREST DURING THE FIRST DECADE SINCE  
PLANTATION ON A FORMER CROPLAND**

**CARBON, WATER, AND ENERGY DYNAMICS OF A TEMPERATE  
PINE FOREST DURING THE FIRST DECADE SINCE  
PLANTATION ON A FORMER CROPLAND**

By

Felix Chung Chung Chan, B.Sc.

A Thesis

Submitted to the School of Graduate Studies

In Partial Fulfillment of the Requirements

For the Degree

Master of Science

McMaster University

© Copyright by Felix Chun Chung Chan, April 2016

**MASTER OF SCIENCE (2016)**  
**(School of Geography and Earth Sciences)**

**MCMASTER UNIVERSITY**  
**HAMILTON, ON**

**TITLE:** Carbon, water, and energy dynamics of a temperate pine forest during the first decade since plantation on a former cropland

**AUTHOR:** Felix Chun Chung Chan  
B.Sc. (Hons) (McMaster University)

**SUPERVISOR:** Dr. M. Altaf Arain

**NUMBER OF PAGES:** xi; 79

## ABSTRACT

This study presents the energy, carbon (C), and water exchange dynamics of a recently afforested temperate white pine (*Pinus strobus* L.) forest, established on former agricultural land in 2002, in southern Ontario, Canada during the initial thirteen years (2003–2015). Our observations show that the forest became a consistent sink of C after only 5 years of its establishment (ranging from 105 g C m<sup>-2</sup> to 216 g C m<sup>-2</sup> between 2008 to 2015), owing to sandy soils and low residual soil organic matter from prior agricultural activities. This region frequently experiences low precipitation (P) and soil moisture (VWC) limitations and/or heat stress in late summer, causing a reduction in net ecosystem productivity (NEP). Seasonal and annual dynamics of NEP showed reduced C uptake during years with heat and/or drought events (i.e. 2007 and 2012). In 2007, the impact of a seasonal drought was much more exacerbated when combined with a heatwave, resulting in a strong C source. Similarly, the inter-annual variability of evapotranspiration (ET) gradually increased with stand age (mean 370 mm yr<sup>-1</sup>) and water use efficiency (WUE) consistently increased (mean 2.65 g C kg<sup>-1</sup> H<sub>2</sub>O). Quantum yield,  $\alpha$  (0.019 to 0.045) and maximum photosynthetic capacity,  $A_{\max}$  (4.37 to 33.6  $\mu\text{mol m}^{-2}\text{s}^{-1}$ ) increased steadily as the size and density of the canopy increased with stand age. Energy fluxes were influenced by canopy development as net radiation (R<sub>n</sub>), latent heat (LE), and sensible heat (H) flux increased, while ground heat flux (G) peaked in 2007 and then gradually declined. Our analysis showed that daily C fluxes are primarily driven by R<sub>n</sub> and temperature (T<sub>s</sub>, T<sub>a</sub>) which explained 47%, 61%, 52%, and 68% of the variability in gross ecosystem productivity (GEP), ecosystem respiration (RE), NEP, and ET. This study is a significant contribution to our understanding of the energy, C, and water dynamics of young planted conifer forests and controls on their growth and C uptake. Our findings demonstrate the potential of utilizing white pine as a means to sequester atmospheric CO<sub>2</sub> in southern Ontario and other regions of North America with similar climate and site history.

## **ACKNOWLEDGEMENTS**

First and foremost, I would like to thank my supervisor and “academic father”, Dr. Altaf Arain for being kind-hearted, patient, and supportive throughout my time as a Masters student. I will always appreciate the opportunity you gave me to explore my passion for forests and to leave my mark on the world through research.

Secondly, I would like to extend a heartfelt thanks to the Hydromet family – it’s become an absolute pleasure spending time with you in the office and field. Rob – thank you for your continued guidance in the field and always being just a phone call away. Your sense of pragmatism never ceases to amuse me. Myroslava – thank you for inspiring me with your unwavering optimism and resourcefulness. Jay – thank you for being an encyclopedia of knowledge and helping with any data-related inquiries. Rachel – thank you for setting the bar on academic achievements. Hussein – thank you for your guidance in the statistical realm. Shawn, Katey, Jung, Eric, Brandon, and Olivier – words cannot express my gratitude for the comradery we have built. Additionally to those in the School of Geography and Earth Sciences, some of whom are my closest friends, your warmth and support through social gatherings and intermural sports is greatly appreciated.

I would like to acknowledge: Zoran Nestic from the Biometeorology and Soil Physics Group at the University of British Columbia for technical support in flux measurements and instrumentation. Dr. Jing Chen’s Remote Sensing and GIS Lab at the University of Toronto, particularly Holly Croft who provided LAI measurements. Steve Williams and Ken Elliott from OMNR, Dave Holmes and Paul Gagnon from LPRCA for their help. Bruce Whitside for providing access to his private forest to conduct this research.

Lastly, I would like to dedicate this work to my parents, whose sacrifices allowed me to pursue the environmental sciences. It is my sincere hope that the implications of this research can bring about positive change that they can be proud of.

## TABLE OF CONTENTS

|  |      |
|--|------|
| Abstract .....   | iii  |
| Acknowledgements .....   | iv   |
| Table of Contents .....  | v    |
| List of Tables .....   | vii  |
| List of Figures .....  | viii |
| List of Abbreviations .....  | x    |
| Chapter 1: Introduction .....  | 1    |
| 1.1 Forest Ecosystems .....  | 1    |
| 1.2 Forests and Climate Change .....   | 2    |
| 1.4 Plantation Forests .....   | 4    |
| 1.5 Eastern white pine in southern Ontario .....                                     | 5    |
| 1.6 Quantification of carbon exchange with the eddy covariance technique .....       | 7    |
| 1.7 Research Objectives .....  | 8    |
| Chapter 2: Literature Review .....   | 10   |
| 2.1 Use of Chronosequence Synthesis studies to predict Carbon trajectories .....     | 10   |
| 2.2 Age-related differences of carbon fluxes in plantation and natural forests ..... | 13   |
| 2.3 Environmental Controls on Carbon Fluxes .....                                    | 14   |
| 2.3.1 Light Quality .....  | 14   |
| 2.3.2 Temperature .....  | 15   |
| 2.3.3 Water .....  | 16   |
| 2.3.4 Age dependent controls .....   | 16   |
| Chapter 3: Methodology .....   | 19   |
| 3.1 Study site .....   | 19   |
| 3.2 Flux and micrometeorological measurements .....                                  | 20   |
| 3.3 Data processing and gap-filling .....  | 21   |
| 3.3.1 Micrometeorological Data .....   | 22   |

|  |    |
|--|----|
| 3.3.2 Flux Data .....  | 22 |
| 3.4 Biometric Measurements.....                              | 25 |
| 3.5 Canopy Leaf Area Index .....                             | 26 |
| 3.6 Data Analysis .....                                      | 27 |
| Chapter 4: Results .....                                     | 28 |
| 4.1 Stand Development and Growth .....                       | 28 |
| 4.2 Energy Dynamics in the First Decade since Planting ..... | 28 |
| 4.3 Carbon Dynamics in the First Decade since Planting ..... | 30 |
| 4.4 Water Dynamics in the First Decade since Planting .....  | 32 |
| 4.5 Climatic Controls .....                                  | 33 |
| Chapter 5: Discussion .....                                  | 35 |
| 5.1 Stand Development and Growth .....                       | 35 |
| 5.2 Energy Dynamics in the First Decade since Planting ..... | 36 |
| 5.3 Carbon Dynamics in the First Decade since Planting ..... | 37 |
| 5.4 Water Dynamics in the First Decade since Planting .....  | 39 |
| 5.5 Interactions with Climate .....                          | 41 |
| Chapter 6: Conclusion.....                                   | 44 |
| Chapter 7: Future Works.....                                 | 46 |
| References .....   | 47 |
| Tables .....   | 54 |
| Figures.....   | 59 |
| Supplementary Tables.....                                    | 78 |

## LIST OF TABLES

|         |  |    |
|---------|--|----|
| Table 1 | Site characteristics for TP02.   | 54 |
| Table 2 | Stand biometrics of TP02   | 55 |
| Table 3 | Summary of annual (A) and growing season (GS) meteorological variables.  | 56 |
| Table 4 | Summary of annual (A) and growing season (GS) carbon and evapotranspiration fluxes.  | 57 |
| Table 5 | Water use efficiency (WUE; $\text{g C kg}^{-1} \text{H}_2\text{O}$ ) from the daily GEP and ET relationship. $\alpha$ and $A_{\text{max}}$ values for the best-rectangular hyperbolic curve fitted onto the GEP and PARd relationship. | 58 |

## LIST OF FIGURES

|           |  |    |
|-----------|--|----|
| Figure 1  | Components of an eddy flux.  | 59 |
| Figure 2  | Location of four FLUXNET-associated tower sites in southern Ontario.   | 60 |
| Figure 3  | The half-hourly energy balance of the white pine forest plantation from 1 January 2003 to 31 December 2015.  | 61 |
| Figure 4  | Progress of vegetation growth at TP02 over the past 13 years.  | 62 |
| Figure 5  | Measures of tree growth over the past 13 years.  | 63 |
| Figure 6  | Daily meteorological values at TP02 from 1 January 2003 to 31 December 2015.   | 64 |
| Figure 7  | Seasonal ground heat flux (G); mean annual air ( $T_a$ ) and soil ( $T_{s20cm}$ ) temperature at TP02; the difference between mean annual $T_a$ and $T_{s20cm}$ at TP02 and TP39.  | 65 |
| Figure 8  | Seasonal energy flux of net radiation (Rn); mean monthly upwelling photosynthetically active radiation (PARup); and monthly upwelling longwave radiation ( $L_u$ ).  | 66 |
| Figure 9  | Seasonal energy fluxes of latent heat (LE) and sensible heat (H).  | 67 |
| Figure 10 | Annual carbon fluxes; mean daily volumetric water content (VWC); daily net ecosystem production (NEP); and daily evapotranspiration (ET).  | 68 |
| Figure 11 | A rectangular hyperbolic curve $\left(GEP = \frac{\alpha PARd A_{max}}{\alpha PARd + A_{max}}\right)$ fitted to bin-averaged ( $10 \mu\text{mol m}^{-2}\text{s}^{-1}$ ), half-hourly data gross ecosystem productivity (GEP) and photosynthetically active radiation | 69 |

(PARd).

|           |  |    |
|-----------|--|----|
| Figure 12 | Monthly and annual box plots of daily fluxes of NEP, RE, GEP, and ET fluxes.                           | 70 |
| Figure 13 | Monthly cumulative (a) NEP and (b) ET.   | 71 |
| Figure 14 | Daily water use efficiency (WUE), represented by the slope of C assimilated (GEP) and water lost (ET). | 72 |
| Figure 15 | Variable factor maps from principle component analysis.  | 73 |
| Figure 16 | Main effect plots of linear regression analyses.   | 74 |
| Figure 17 | Observed versus modeled plots of NEP, RE, GEP, and ET fluxes.  | 75 |
| Figure 18 | Residual plots of (a) NEP, (b) RE, (c) GEP, and (d) ET models.   | 76 |
| Figure 19 | Comparison of NEP in young stands across North America.  | 77 |

## **LIST OF ABBREVIATIONS**

CO<sub>2</sub> = Carbon dioxide

C = Carbon

NEE = Net ecosystem exchange

NEP = Net ecosystem productivity

GEP = Gross ecosystem productivity

RE = Ecosystem respiration

ET = Evapotranspiration

WUE = Water use efficiency

$\alpha$  = Quantum yield

A<sub>max</sub> = Photosynthetic capacity

Rn = Net radiation

LE = Latent heat flux

H = Sensible heat flux

G = Ground heat flux

LAI = Leaf area index

Dbase = Diameter at base height

DBH = Diameter at breast height

IPCC = International Panel on Climate Change

EC = Eddy covariance

OPEC = Open-path eddy covariance

CPEC = Closed-path eddy covariance

TPFS = Turkey Point flux station

$T_a$  = Air temperature

$T_s$  = Soil temperature

PARd = Downwelling photosynthetically active radiation

PARup = Upwelling photosynthetically active radiation

$L_u$  = Upwelling terrestrial longwave radiation

VPD = Vapour pressure deficit

VWC = Volumetric water content

P = Precipitation

## **CHAPTER 1: INTRODUCTION**

### **1.1 Forest Ecosystems**

Forest ecosystems currently cover the largest amount of ice-free land surface among all terrestrial ecosystems (Waring and Running, 2007). They provide vital ecosystem services including production of freshwater from mountain watersheds, cleanse the air of pollutants, support wildlife, and provide recreational opportunity. A large fraction of forested land has been converted for agricultural and urban usage. With a growing human population and propensity for a higher standard of living, the importance of the world's remaining forests are likely to continue to increase as well as the challenge to manage and sustain them as resources (Waring and Running, 2007).

Forests are comprised of trees, woody perennials with a single main stem radiating branches, twigs, and foliage to form a crown (Smith et al., 2009). Tree stems consist mainly of support and transport tissues. The xylem transports water and nutrients up from the roots to the branches and leaves. In turn, the phloem transports sugars (carbohydrates) produced from leaf photosynthesis to all other living tissues (Smith et al., 2009). There are four major classifications of trees. Evergreen trees remain green during the dormant season since all leaves do not drop simultaneously and the trees are never leafless (Lorenz and Lal, 2010). Deciduous trees experience leaf senescence at the end of the growing season, in which all leaves are shed. Coniferous trees or conifers are cone-bearing, whereas all non-cone bearing but flower-bearing trees are called broad-leaved trees. Conifers have needle-shaped leaves whereas flowering trees have broad or flattened leaves (Lorenz and Lal, 2010). Trees which produce seeds that are essentially naked are called gymnosperms whereas those enclosed within a fruit body are called angiosperms (Smith et al., 2009).

Forest ecosystems include all living components of the forest and its boundaries extend vertically upward into the atmospheric layer surrounding the forest canopy and downwards into the lowest soil layers affected by roots and biotic processes (Waring and

Running, 2007). Ecosystem ecology focuses on the contribution that a collective of species makes to the water, carbon, energy, and nutrient transfer on the landscape. For example, an ecosystem ecologist describes forest growth as net primary production (NPP) in grams of carbon per m<sup>2</sup> per year (g C m<sup>-2</sup> yr<sup>-1</sup>), as opposed to concentrating on the growth of individual trees. Forest ecosystems are open systems that exchange energy and matter (e.g. CO<sub>2</sub>, H<sub>2</sub>O) with other systems, including adjacent forests, aquatic ecosystems, and the atmosphere. This renders a forest ecosystem never in equilibrium (Waring and Running, 2007).

## **1.2 Forests and Climate Change**

Atmospheric carbon dioxide (CO<sub>2</sub>) concentration has increased by 40% from 280 to 400 ppm since 1750, concentrations which have not been observed in the past 800,000 years (Bala, 2013; IPCC, 2014). CO<sub>2</sub> concentrations observed the fastest decadal rate of change ( $2.0 \pm 0.1 \text{ ppm yr}^{-1}$ ) from 2002 – 2011. Between 1750 and 2011, anthropogenic CO<sub>2</sub> emissions totaled  $2040 \pm 310 \text{ Gt CO}_2$  with approximately half of it occurring from 1970 onwards (IPCC, 2014). During this period, there was a warming effect of  $2.3 \text{ Wm}^{-2}$  from radiative forcing in which CO<sub>2</sub> was the largest contributor. The largest sources of CO<sub>2</sub> emissions are from fossil fuel combustion, cement production, and flaring, followed by forestry and other land use (FOLU) (IPCC, 2014). Although sinks are able to remove CO<sub>2</sub> from the atmosphere and store them in natural carbon cycle reservoirs, approximately 40% ( $880 \pm 35 \text{ Gt CO}_2$ ) of these anthropogenic CO<sub>2</sub> emissions still reside in the atmosphere (IPCC, 2014). The period from 1983 – 2012 was very likely the warmest 30-year period in the last 800 years in the Northern Hemisphere (IPCC, 2014). Furthermore, each successive decade was warmer than any preceding decade since 1850. From 1880 – 2012, globally averaged combined land and ocean surface temperatures have increased linearly by  $0.85^\circ\text{C}$  (IPCC, 2014). Ecosystems and many human systems have become significantly vulnerable and exposed to the impacts of climate-related extreme events (e.g. heat waves, droughts, floods) under current climate variability. The

risks associated with these extreme events are expected to increase progressively with further climate warming (IPCC, 2014). Following the adoption of the Paris Agreement in 2015, Canada will be required to increase its mitigation efforts to reduce CO<sub>2</sub> emissions to constrain the global temperature rise well below 2°C and to drive efforts to limit the increase to 1.5°C (United Nations, 2015).

The rate of increase in atmospheric CO<sub>2</sub> can be reduced through carbon (C) sequestration into various terrestrial components. The IPCC defines C sequestration as the natural transfer of atmospheric CO<sub>2</sub> into long-lived pools (i.e. ocean, biosphere, pedosphere, geosphere) that would otherwise be emitted or remain in the atmosphere (IPCC, 2007). Exchange with the atmospheric CO<sub>2</sub> pool is of great importance to the short-term C cycle in forest ecosystems (Lorenz and Lal, 2010). C sequestration in forest ecosystems primarily occurs by uptake of atmospheric CO<sub>2</sub> during tree photosynthesis and the subsequent transfer of some fixed C into vegetation, detritus, and soil pools for secure C storage (Lorenz and Lal, 2010). Enhancing C sequestration by increasing forested land area (i.e. afforestation) is one of the most cost-effective options to mitigate elevated atmospheric CO<sub>2</sub> levels and hence contribute towards the prevention of global warming (IPCC, 2014, 2005).

Throughout the forest life cycle, assimilatory and respiratory C flux capacity change in magnitude as forests undergo physiological changes as well as changes in growth and decomposition rates (Peichl et al., 2010a). If an ecosystem has a net gain of CO<sub>2</sub> from the atmosphere, it is a sink of C. An ecosystem becomes a source if there is a net loss of CO<sub>2</sub> to the atmosphere. Various chronosequence and synthesis studies investigating age effects suggest that forest stands of burn and harvest origin are typically shown to be sources of C during the initial years, eventually becoming C neutral, and then C sinks as they reach maturity (Amiro et al., 2006; Clark et al., 2004; Coursolle et al., 2012; Zha et al., 2009). However, the reported timing of maximum productivity varied among studies by several decades, even among the same plant functional types (Peichl et al., 2010a). In addition, the age of transition from a C source to C sink is quite variable, depending upon

climate, site history, site management, and disturbance history. For example, Amiro et al. (2010) found that ecosystems subject to a stand replacing disturbance events became a C sink in 10 to 20 years. Thornton et al. (2002) reported that evergreen needleleaf forests in the U.S. became C sinks between 4 and 16 years.

Globally, forests contain approximately 45% of the surface C stock, while the majority is found in forest soils (Jarvis et al., 2005). The temperate forest biome stores 73 to 159 Pg C in vegetation and 153 to 195 Pg C in soil (1 m depth) (Lorenz and Lal, 2010).

Estimates for the boreal and tropical biomes, respectively, are 78 to 143 and 206 to 389 Pg C in vegetation and 338 and 214 to 435 Pg C in soils (1 m depth). Soil organic C (SOC) primarily sequesters C from belowground inputs from vegetation and detritus. The average ratio of soil C to vegetation C ranges from 5:1 in boreal, 2:1 in temperate, to 1:1 in tropical forests. Thus, changes in soil C stocks are equal or greater in importance than changes in vegetation C stocks (Jarvis et al., 2005; Lorenz and Lal, 2010). The efficiency of C sequestration varies among the 100,000 tree species that vary in growth, mortality, decomposition, and climate (Lorenz and Lal, 2010). Estimates of annual C uptake are 0.49 to 0.7 Pg C for the boreal, 0.37 Pg C for the temperate, and 0.72 to 1.3 Pg C for the tropical forest biome. However, there is a lack of biome data in regards to forest stands of all species at all stages of the life cycle, from regeneration to harvest. Thus, estimates of C sequestration and C budgets in forest biomes are uncertain (Lorenz and Lal, 2010).

#### **1.4 Plantation Forests**

As previously mentioned, plantations serve as effective biological sinks of CO<sub>2</sub> since approximately 50% of plant structural matter consists of C derived from atmospheric CO<sub>2</sub> (West, 2014). When plantations are established for environmentally beneficial purposes, it is hoped that they will also provide wood products as well. Across the world, plantations are largely grown to produce wood for industrial use primarily in building or paper production (West, 2014). The majority of these plantations are grown for 10-50

years before harvesting. In forestry, this is known as a rotation – the period from planting to final harvest (West, 2014). Wood utilized as building material may last hundreds of years before being discarded as waste and subsequently release CO<sub>2</sub> in decomposition. Plantations and wood residues, by-products of harvesting and processing, are also used in bioenergy production, by feeding boilers that generate electricity or producing ethanol through fermentation (West, 2014). This has lead plantations to be considered a C neutral commodity, since their initial uptake and eventual release of CO<sub>2</sub> are equivalent. This contrasts fossil fuels, which contribute additional CO<sub>2</sub> to the atmosphere by releasing C stored millions of years ago (West, 2014).

### **1.5 Eastern white pine in southern Ontario**

Worldwide, pines (members of the genus *Pinus*) are the most prominent plantation species, comprising of about 35% of plantation area (West, 2014). In eastern North America, white pine (*Pinus strobus* L.) are considered one of the most productive, fast-growing species that can reach heights of 45 to 60 m (Kula, 2013; Peichl and Arain, 2006). White pine typically has an intermediate shade tolerance that diminishes with age (Abrams, 2001), with a lifespan ranging from 350 to 400 years (Kula, 2013). It is able to occupy a wide range of soil, moisture, and disturbance conditions (Abrams, 2001). Optimal growth occurs in dry environments with well-drained, nutrient-poor, sandy soils (Abrams, 2001; Arain and Restrepo-Coupe, 2005). White pine is a disturbance-dependent species that establishes after small to moderate-scale disturbances such as fire and blow-down, or invasion of abandoned farmland (Abrams, 2001). White pine can recruit into early to middle successional stages by exploiting gaps created during periodic disturbances, eventually facilitating the return of native species (Parker et al., 2001). Additionally, white pine can recruit into late successional to climax stages however it seldom occurs due to the relatively low frequency of disturbance (Abrams, 2001). The multitude of pathways in species recruitment, forest development, and successional

changes presented white pine with plenty of opportunities to thrive in the presettlement forest (Abrams, 2001).

In Southern Ontario, eastern white pine (*Pinus strobus* L.) has been historically valued as a lightweight building material, readily accessible along river banks with light, sandy soils (Abrams, 2001). Settlement of the region in the 18<sup>th</sup> and 19<sup>th</sup> centuries initiated heavy logging and clearing of forests for agriculture, resulting in the removal or modification of old-growth forests (Parker et al., 2001). A comparison of pre-European settlement and modern forest composition of white pine shows an overall decline in northeastern and Great Lake states in the United States (Abrams, 2001). Presently, the highly productive white pine is valued for its potential to sequester C and/or provide quality wood products that are considered C neutral. Due to its wide range of applications and growing conditions, the prevalence of white pine as a plantation species has re-emerged in eastern North America.

## 1.6 Quantification of carbon exchange with the eddy covariance technique

Eddy covariance (EC) is one of the most direct and defensible ways to measure ecosystem carbon exchange (Burba and Anderson, 2010), as well as water vapour and energy fluxes. Since the late 1980s, the EC method has been widely used by micrometeorologists, ecologists, and other environmental scientists. It is based on the theory of turbulent transport, in which eddies, rotating air parcels, are produced by turbulent flow in the surface layer of the atmosphere. Each eddy has 3-D components, including a vertical wind component (**Figure 1**). The vertical flux is represented as the covariance between vertical wind speed and the gas concentration.

The EC method provides an *in situ* and direct estimate of gas and energy fluxes between the atmosphere and underlying vegetation surface without ground disturbance (Baldocchi et al., 2001). Forest scientists attach EC and meteorological instruments to either walk-up scaffolding or low-profile radio towers to measure spatially averaged fluxes of relatively large areas of land (100–2000m in length). The spatial scope of this method has been expanded with networks of measurement sites, such as the Ameriflux and the Global Fluxnet Network. This allows researchers to quantify how whole ecosystems respond to a spectrum of climate regimes (Baldocchi et al., 2001). There are several important assumptions: (1) the terrain must be horizontal and uniform; (2) atmospheric conditions must be steady; and (3) the underlying vegetation sampled (the flux footprint) extends horizontally upwind for an adequate distance, usually about 100 times the sampling height (Baldocchi et al., 2001; Baldocchi, 2003). Systematic errors will result in the interpretation of EC data if these assumptions are violated. When thermal stratification of the atmosphere is stable or turbulent mixing is weak (e.g. nighttime), CO<sub>2</sub> exiting the leaves and soil may not reach the height of the instruments above the canopy, resulting in an underestimate of ecosystem respiration (RE) by the EC method. Under such conditions, the storage term becomes non-zero and must be added to the EC measurements to represent within-canopy C balance (Baldocchi et al., 2001; Baldocchi, 2003). The net exchange of CO<sub>2</sub> between the ecosystem and the atmosphere is known as

net ecosystem exchange (NEE). In simplified terms, NEE is calculated as  $F_c + \Delta S_c / \Delta t$ , where  $F_c$  is the EC flux of  $\text{CO}_2$ ,  $\Delta S_c$  is the rate of change in  $\text{CO}_2$  storage within the air column below the EC sensor, and  $\Delta t$  is the period of time. The net ecosystem productivity (NEP) is given by  $-NEE - F_{\text{DOC}} \approx -NEE$ , where  $F_{\text{DOC}}$  represents the leaching of dissolved organic carbon (DOC) from the root zone, which is considered negligible over a short time period.

Non-closure of the energy balance usually results when assumptions are not upheld. Forest energy balance closure is calculated by comparing turbulent fluxes ( $H+LE$ ) and available energy ( $Rn-G+S$ ). A cross-site evaluation by Wilson et al. (2002) suggests that 22 sites of varying vegetation types and climates had a mean imbalance of 20%. The imbalance was greatest during the night. They suggest that estimates of turbulent fluxes of sensible heat ( $H$ ), latent heat ( $LE$ ), and net ecosystem exchange ( $NEE$ ) were underestimated and/or available energy was overestimated. Correction factors may be applied to errors associated with the EC method or calculations for the available energy terms (Wilson et al., 2002). Nevertheless, the strengths of the EC method outweigh the weaknesses, as EC flux towers can provide long-term, continuous, half-hourly measurements of energy,  $\text{CO}_2$ , and  $\text{H}_2\text{O}$ .

## 1.7 Research Objectives

To date, only a few decadal-long  $\text{CO}_2$  flux studies have been published (e.g. a mature boreal black spruce site: Dunn et al., 2007; a mature Pacific Northwest Douglas-fir site: Chen et al., 2009; young sub-tropical slash pine plantations: Bracho et al., 2012). To our knowledge, no decadal-scale  $\text{CO}_2$  flux studies have been reported for afforested or plantation stands. This study reports the initial 13 years of eddy covariance fluxes (2003–2015) of an afforested white pine forest, established on an abandoned agricultural land in 2002, near Walsingham, Ontario, Canada. The main objective of this study was to examine how energy, C, and water fluxes vary during the first decade of land-use change,

when converting an abandoned cropland to a forested land. The observations will allow the characterization of the length of time it takes for an afforested stand to turn from a source of C to a sink of C. The secondary objective was to investigate key climatic variables that drive carbon fluxes at this forest site and how their impact changes in the first decade of stand development.

## **CHAPTER 2: LITERATURE REVIEW**

### **AGE EFFECTS AND ENVIRONMENTAL CONTROLS ON CARBON FLUXES IN NORTH AMERICAN CONIFER FORESTS**

#### **2.1 Use of Chronosequence Synthesis studies to predict Carbon trajectories**

To study the long-term dynamics of ecosystems from decadal to millennial time-scales, ecologists frequently use the chronosequence method. A chronosequence is a space-for-time substitution, which assumes that different sites, which are similar except in age since some initiating disturbance, can be considered a time sequence (Johnson and Miyanishi, 2010). The key assumptions of chronosequences are that: (1) sites of different ages are following the same trajectory, in that younger sites are currently undergoing the same development that the older sites experience (Walker et al., 2010) and (2) each site had the same initial conditions (Johnson and Miyanishi, 2010). Thus, chronosequences can be used to study forest ecosystems that follow the same trajectory, have low biodiversity, rapid species turnover, and low frequency and severity of disturbance (Walker et al., 2010).

In North America, most chronosequence studies were conducted under the Fluxnet Canada Research Network, AmeriFlux, and/or the North American Carbon Program. Several synthesis studies have quantified successional patterns of NEP after disturbance. Coursolle et al. (2012) estimated the C flux trajectories of harvested jack pine (HJP-SK) (see Zha et al., 2009) and burned jack pine (BJP-SK) in Saskatchewan, harvested black spruce in Quebec (HBS-QC) (see Payeur-Poirier et al., 2012), burned black spruce (BBS-MB) in Manitoba (see Goulden et al., 2011), harvested Douglas-fir (HDF-BC) in British Columbia (see Schwalm et al., 2007), and afforested white pine (TPFS) in Ontario (see Peichl et al., 2010). Amiro et al. (2010) investigated C fluxes of North American forests after disturbance using chronosequences of fire, harvest, insect, and storm origin. Thornton et al. (2002) investigated C fluxes in evergreen needleleaf forests in the continental United States.

Estimates of NEP from curve fitting indicate that boreal forests in Canada become C sinks in 10 years and offset initial C losses after 26 years (Coursolle et al., 2012).

Estimates from temperate chronosequences indicate that the harvested Douglas-fir and afforested white pine stands become sinks of C in 18 and 3 years and offset initial C losses after 47 and 4 years of growth. Previous studies conducted in these chronosequences predicted the C compensation point to range from 10 to 20 years (Schwalm et al., 2007; Zha et al., 2009). Amiro et al. (2010) demonstrated that chronosequences across North America become C sinks within 10 to 20 years, regardless of disturbance type. Thornton et al. (2002) predicted needle-leaf forests to become sinks ranging from 4 years post-harvest to 16 years post fire.

The speed of recovery after disturbance or planting is suggested to depend on the speed of GEP recovery against a background level of heterotrophic respiration (Rh) (Giasson et al., 2006). Any forest management practice that reduces the magnitude of Rh associated with the disturbance will propel the ecosystem to reaching a positive NEP quicker (Pregitzer and Euskirchen, 2004). The PWP-ON plantations, including the site reported in this study were established in abandoned agricultural fields, likely containing low residual soil C resulting in significantly lower RE rates (Peichl et al., 2010a). It is this low soil C pool that allowed the PWP-ON stands to have higher NEP rates and reach the compensation point in only 3 years, in contrast to the high productive HDF-BC stands that likely had higher soil C pools after harvest. Bracho et al. (2012) reported similarly high rates of NEP and a C compensation point of 4 years in Florida slash pine plantations, established over previous plantations with stumps left in place. It is important to note however, that the stand was a strong C source with a 3-year mean of  $-550 \text{ g C m}^{-2}$  before becoming a C sink.

Coursolle et al. (2012) showed that the NEP of HJP-SK and BBS-MB to peak at  $98 \pm 30$  and  $149 \pm 40 \text{ g C m}^{-2} \text{ yr}^{-1}$  at ages 40 and 55. HDF-BC and PWP-ON peaked at  $292 \pm 100$  and  $694 \pm 66 \text{ g C m}^{-2} \text{ yr}^{-1}$  at ages 47 and 17. Peak NEP coincided with peak leaf area index (LAI). These findings correspond with those of Pregitzer and Euskirchen (2004),

who reported the age range of 31 to 120 years for peak NEP to occur in the boreal biome. However, their suggested range of 11 to 30 years in the temperate biome does not coincide with HDF-BC. Thornton et al. (2002) simulated peak NEP to occur 2 to 7 years after the C compensation point, ranging from 8 to 19 years.

Although boreal forest stands typically have larger soil C to vegetation C ratio, their losses range from  $370 \pm 180 \text{ g C m}^{-2}$  at BBS-MB to  $1220 \pm 80 \text{ g C m}^{-2}$  at HJP-SK before becoming C sinks, while the temperate HDF-BC and PWP-ON stands lose  $6030 \pm 250$  and  $210 \pm 150 \text{ g C m}^{-2}$  (Coursolle et al., 2012). The greatest C loss in the initial years after harvesting occurred at warmer sites, which had a greater interannual variability than colder sites (Amiro et al., 2010). There is also a fundamental difference between harvest and fire chronosequences. In burned stands, fire removes the fine materials and leaves the coarse woody material. Rh would likely not increase until snags make contact with the ground, become moist, and decay (Amiro et al., 2006). In harvested stands, much of the coarse material is removed, likely resulting in greater Rh during the early years until the finer material decomposes. Initial respiration losses from woody debris is instrumental in determining the successional patterns for NEP during early development (Peichl et al., 2010a). Thornton et al. (2002) predicted that evergreen needleleaf forests located in warmer climates of continental US released 1490 to 3040  $\text{g C m}^{-2}$  before becoming C sinks. Coursolle et al. (2012) project net C gain at 80 years to be  $3810 \pm 220$  to  $8190 \pm 340 \text{ g C m}^{-2}$  in boreal forests,  $8630 \pm 1210 \text{ g C m}^{-2}$  in HDF-BC, and  $27000 \pm 650 \text{ g C m}^{-2}$  in afforested PWP-ON. However, these projections, especially in HDF-BC and PWP-ON, may be uncertain due to a lack of data points in certain age ranges (Coursolle et al., 2012).

It is worth discussing that PWP-ON stands were anomalies in the synthesis study, which comprised of mostly low productivity boreal forest sites. Coursolle et al. (2012) noted that there was an absence of age effect on  $SL_{GEP}$  (growing season length derived from GEP thresholds) due to differences in ground cover properties and site management among the chronosequence. Peichl et al. (2010) noted that PWP-ON stands do not exhibit

typical age-related patterns in C fluxes. In their study, C fluxes measured by the EC method were normalized by a site index (SI), a forestry practice not applied to EC fluxes generally in literature. SI is a measure of site quality based on a species-specific relationship between the height of the dominant trees and base age. Peichl et al. (2010) demonstrated that site quality affects the interpretation of age-related C flux in forests chronosequences. Thus, SI-normalization is a simple and efficient way to identify age-related patterns in C fluxes in forest chronosequence studies and to improve large-scale estimates of C.

## **2.2 Age-related differences of carbon fluxes in plantation and natural forests**

Arain and Restrepo-Coupe (2005) compared 20 temperate conifer forests from across the globe, of which 11 were plantation forests and 9 were naturally regenerating stands originating from fire or harvest. Only the 65 year-old white pine plantation from PWP-ON was included at the time. The majority of forests did not exceed 100 years-old, and were C sinks on an annual basis ranging from 5 to 760 g C m<sup>-2</sup> yr<sup>-1</sup> (Arain and Restrepo-Coupe, 2005). An intensively managed Sitka spruce plantation in Griffith, UK had the greatest NEP of 620 g C m<sup>-2</sup> yr<sup>-1</sup>. Maximum GEP of 2085 g C m<sup>-2</sup> yr<sup>-1</sup> was observed at the 55 year-old Douglas-fir plantation from HDF-BC, although the previously discussed high RE resulted in a low NEP of 360 g C m<sup>-2</sup> yr<sup>-1</sup>. Among the natural forests, the 140 year-old Norway spruce stand in Tharandt, Germany had the highest NEP of 525 g C m<sup>-2</sup> yr<sup>-1</sup>, followed by 270 g C m<sup>-2</sup> yr<sup>-1</sup> in a mixed-aged ponderosa pine stand in Oregon, US. The Wind River old-growth stand in Washington, US was a C source at -95 g C m<sup>-2</sup> yr<sup>-1</sup> (Arain and Restrepo-Coupe, 2005).

Carbon uptake in plantation stands diminished with stand age up to 100 years, as GEP declined linearly whereas RE decreased little (Arain and Restrepo-Coupe, 2005). In natural stands, NEP was observed to rise with stand age up to 100 years, owing to a steady increase of both GEP and RE. When they exceeded 100 years, NEP declined with

age. Thus, photosynthesis, rather than respiration is shown to dictate the carbon uptake of both plantation and natural forests (Arain and Restrepo-Coupe, 2005). Overall, C fluxes of plantation stands of 0 to 100 years were much higher, particularly those in early developmental stages. Although tree density declines with age in both plantation and natural stands, high density causes young plantations to experience higher GEP and RE. This is likely due to greater leaf and root biomass. Young plantations are also subject to various treatments before planting which may contribute to high RE values (Arain and Restrepo-Coupe, 2005).

## **2.3 Environmental Controls on Carbon Fluxes**

Multi-site regional and global analyses have been used to investigate the influence of environmental and/or structural variables on C exchanges in forests. Law et al. (2002) investigated environmental controls of CO<sub>2</sub> using data from Fluxnet sites representing various plant functional types and climatic zones. They discussed three major controls: light quality, temperature, and water.

### *2.3.1 Light Quality*

For a given solar elevation, the highest solar irradiance occurs on partly cloudy days, not clear days (Law et al., 2002). The ‘cloud gap effect’ increases the amount of incident diffuse radiation due to light scattering and reflection of clouds in the vicinity (Oke, 1987). Thus, cloud cover results in a greater proportion of diffuse radiation and a higher fraction of light penetrating the lower depths of the canopy. NEP was found to be greater under cloudy conditions in a boreal Scots pine forest, when evaluated in relationship to diffuse versus direct PARd (Law et al., 2002). This may have been due to a more efficient distribution of non-saturating light conditions for photosynthesis, lower vapour pressure deficit (VPD) limitation to photosynthesis, and lower respiration associated with reduced temperature. Since stomatal conductance ( $g_s$ ) is a function of available water and evaporative demand, low VPD allows a higher  $g_s$  and thus greater C uptake (Law et al.,

2002). CANVEG model simulations for deciduous forests demonstrate that photosynthesis is a linear function of PAR<sub>d</sub> for shaded leaves and a curvilinear function for sunlight leaves. Although PAR<sub>d</sub> components are addressed separately in models, field measurements of diffuse and direct PAR<sub>d</sub> are lacking (Law et al., 2002).

### 2.3.2 *Temperature*

Soil autotrophs and heterotrophs can comprise of up to 75% of RE (Law et al., 2002). Law et al. (2002) found that at individual sites, short-term RE is correlated with temperature when water availability is not limiting soil processes. When sites were subject to growing season droughts, the influence of air temperature ( $T_a$ ) on RE for individual sites was smaller. Decomposition rates are influenced by site history and recent site disturbance. Generally, boreal forests typically have lower respiration rates due to longer periods of soil wetness, whereas ecosystems at lower latitudes experience periods of soil water deficits that result in higher respiration rates (Law et al., 2002). Law et al. (2002) found poor correlation and relationship between annual RE and mean annual  $T_a$  across all sites (i.e. evergreen coniferous forests, deciduous broadleaf forests, evergreen broadleaf forests, and grasslands). They suggest improving estimates of annual RE with daily and seasonal temperature amplitudes, as well as accounting for long-term heterotrophic decomposition processes. Arain and Restrepo-Coupe (2005) found annual GEP and RE had positive relationships with  $T_a$  in both plantation and natural forests ( $r^2 = 0.57$  and  $0.51$  for GEP and  $r^2 = 0.32$  and  $0.58$  for RE). This is likely because warmer regions showed higher photosynthetic uptake and higher respiratory losses. The weak relationship between RE and  $T_a$  at plantations is due to differences in site characteristics (e.g. stand structure, litter substrate, and management practices) that impact autotrophic and heterotrophic respiration (Arain and Restrepo-Coupe, 2005). Law et al. (2002) determined mean annual  $T_a$  to explain 50% of the variability in GEP across all sites. However, they caution that autocorrelation could arise from the calculation of GEP using NEE and estimated RE (Law et al., 2002). Reichstein et al. (2007) split CARBOEUROFLUX sites located above and below 52°N, separating the boreal and

temperate biomes. Sites located above 52°N had annual GEP and RE correlated with  $T_a$  and sites below 52°N were correlated with available soil moisture. Annual NEP was poorly correlated to  $T_a$ , likely as the photosynthesis and respiration components respond to temperature differently (Law et al., 2002). Photosynthesis is influenced by  $T_a$  and PARd, which fluctuates seasonally with phenology and biochemistry (Law et al., 2002). In addition to temperature and moisture, Rh can be limited by substrate quality and quantity, which can have a large effect on total RE. Arain and Restrepo-Coupe (2005) found a similar lack of relationship within natural stands, whereas annual NEP in plantation stands linearly increased with  $T_a$  ( $r^2 = 0.42$ ).

### 2.3.3 Water

Annual precipitation (P) indicates the moisture status of a site, which impacts LAI and hence GEP (Arain and Restrepo-Coupe, 2005). Soil moisture also affects heterotrophic respiration, which can account for up to 50% of RE. Although warmer temperatures and longer growing seasons can facilitate more C sequestration, water-stress may cause setbacks in forest productivity. Arain and Restrepo-Coupe (2005) show that annual GEP and R have a strong positive relationship with P in both plantation and natural forests ( $r^2 = 0.80, 0.54$  for GEP and  $r^2 = 0.76, 0.65$  for R, respectively). Moist sites had higher GEP and R, suggesting a strong water-availability control on photosynthetic uptake and respiratory losses in temperate conifer forests. P only had a moderate influence on annual NEP, explaining 46% and 34% of variability in plantation and natural forests (Arain and Restrepo-Coupe, 2005). Law et al. (2002) found the annual site water balance ( $\sum(ET - P)$ ) to explain 29% of variability in GEP among forests. However when combined with  $T_a$ , 64% of the variability in GEP was explained. They also reported weak correlations between annual NEP and water balance and  $T_a$  (Law et al., 2002).

### 2.3.4 Age dependent controls

Most recently, Coursolle et al. (2012) addressed this subject by dividing their study sites into age classes, given the strong relationship between C fluxes and stand age. Their

classifications were 73 to 153 years, 23 to 64 years, and 1 to 15 years for mature, intermediate, and young stands respectively. A stepwise regression analysis indicated that mean growing season volumetric soil water content (VWC-GS) and near-surface soil temperature ( $T_s$ ) explained 85% and 86% of the variability in annual GEP and RE, respectively, of mature stands. Mean growing season air temperature ( $T_a$ -GS) explain 44% of the variability in annual NEP. Total above-ground biomass was strongly correlated to all C fluxes (Coursolle et al., 2012).

At intermediate sites, both climate and stand structure were related to C fluxes.  $SL_{GEP}$  (partial  $r^2 = 0.91$  and  $0.89$ ) combined with SWC-GS explained 95% and 94% of the variability in annual GEP and RE.  $T_s$  and  $T_{s0}$  (number of days the soil was frozen) explained 74% of variability in annual NEP (Coursolle et al., 2012). LAI and RAIN-GS (total rainfall during  $SL_{GEP}$ ) were strongly correlated with annual GEP at intermediate sites, while LAI, temperature, snow cover, and RAIN-GS (RE only) were strongly correlated with annual RE and NEP. LAI was also strongly correlated with annual  $T_a$  and  $T_s$ , suggesting that strong correlations between LAI and C fluxes reflect the regional climate differences within the intermediate age group. The temperate stands HDF-BC and PWP-ON were found to have greater LAI and C fluxes (Coursolle et al., 2012). Thus, fluxes of intermediate-aged stands are related to both climate and structure.

At the young sites, a combination of LAI (partial  $r^2 = 0.87$ ) and  $SL_{GEP}$  explained 90% of the variability in annual GEP. There is a very strong correlation between LAI and GEP, which suggests that stand structure is more important than climate in determining GEP fluxes in young stands. Arain and Restrepo-Coupe (2005) suggest that physical and physiological factors play a greater role on net C uptake compared to environmental controls, particularly for young plantations. In turn, 90% of variability in annual RE is explained by snow cover (partial  $r^2 = 0.70$ ), LAI,  $T_s$ , and  $T_a$  (Coursolle et al., 2012). Correlation coefficients with RE suggest that annual RE in young stands is determined by both stand structure and climate. Lastly, Coursolle et al. (2012) found no significant regressions or correlations for annual NEP at young stands.

The site reported in this study is the youngest site of the PWP-ON chronosequence reported from 2003-2007 by Peichl et al. (2010a) and Coursolle et al. (2012). Currently, this site has over a decade of flux data in which fluxes were measured from the beginning of forest plantation to the present day where the canopy is nearly closed. Not only will this allow us to draw better conclusions about the energy, C, and water dynamics of young afforested stands, but the flux measurements can also be put into perspective against forests of similar nature, including some of the aforementioned sites. Thus, this decadal-scale flux study provides great scientific insight into the early life cycle of plantation stands.

## CHAPTER 3: METHODOLOGY

### 3.1 Study site

This study was conducted at the youngest forest site (TP02) of the Turkey Point Flux Station (TPFS) (42°39'41.93"N, 80°33'35.60"W; elevation 200 m), which is part of the Ameriflux and global Fluxnet networks (**Figure 2**). It is also known as CA-TP1 within the global FLUXNET network and PWP-ON in some studies in literature (e.g. Coursolle et al., 2012). It is located approximately 2 km southwest of the town of Walsingham, near Long Point Provincial Park, off the northern shore of Lake Erie in southern Ontario, Canada. The landscape of the region is largely agricultural, scattered with monoculture and mixed deciduous (Carolinian species) and conifer plantation forests.

The forest (white pine; *Pinus strobus* L.) was planted in 2002 on former agricultural land which was abandoned 10 years prior to plantation. The white pine stand is 10 ha, which is surrounded by deciduous stands and woodlots to the south and southwest, in the direction of the prevailing winds. The topography is gently undulating, with slopes between 0.5 and 1.5% (Presant and Acton, 1984). The terrain is relatively flat with the exception of a 5 to 6 m high sand dune in the north side resulting in a slope of 10% facing south (Peichl, 2005). The soil is classified as Brunisolic Gray Brown Luvisol according to the Canadian System of Soil Classification (Presant and Acton, 1984). The soil is composed of approximately 98% sand, 1% silt, and <1% clay, with low soil nitrogen (N; 0.05-0.07%), soil organic carbon (C; 1.0–1.5%) and C:N ratio (11–20) in the 10 cm mineral soil layer. The soil is well-drained with a low to moderate moisture retention capacity. Further site details are given in **Table 1**.

The climate of the region is continental with warm summers and very cold winters. The 30-year mean annual  $T_a$  over the 1981–2010 period was 8.0°C and an annual P was 1036 mm, of which 632 mm falls from April to October and 135 mm falls as snow (Environment Canada Norms at Delhi, ON).

### **3.2 Flux and micrometeorological measurements**

The eddy covariance (EC) technique was used to measure half-hourly fluxes of carbon dioxide ( $F_c$ ), latent heat (LE), and sensible heat (H) between the forest vegetation and the atmosphere (Fluxnet-Canada, 2003). This provided an in-situ and direct quantification of gas and energy fluxes between the atmosphere and underlying surface without ground disturbance. From January 2003 to December 2007, fluxes were measured using an open path EC (OPEC) system mounted at 2 m on a triangular tower and consisting of an infrared gas analyzer (IRGA) (model LI-7500, LI-COR Inc.), a sonic anemometer (model CSAT-3, Campbell Scientific Inc. (CSI), a fine-wire thermocouple, a temperature/relative humidity sensor (model HMP45C, CSI), and a data logger (model CR5000, CSI) (Peichl et al., 2010a). The roving OPEC was circulated among three of our flux research sites in the area, including TP02, at biweekly (2003–2004) and monthly intervals. This resulted in measurements of roughly 1 month per season, with a total of 4 months per year (Peichl et al., 2010a). WPL corrections were applied to the OPEC system in order to derive half-hourly fluxes from 10 minute averages that corrected for variation in air density (Webb et al., 1980).

Since May 2008, continuous flux data has been collected at TP02 by a closed path EC (CPEC) consisting of an IRGA (model LI-7000, LI-COR Inc.) and sonic anemometer (model CSAT3, CSI) installed at 3 m above the ground. The IRGA was placed in a climate control box with a short (4 m) heated sampling tube. In July 2014, a scaffolding tower was erected and the CPEC system was installed at 8 m above the ground. The LI-7000 and LI-7500 IRGAs were calibrated biweekly and monthly, respectively. Further details regarding the operating conditions and calibration of the IRGA are given by Arain and Restrepo-Coupe (2005).

Flux data from both EC systems were recorded at high frequency (20 Hz) and saved onto a desktop computer housed in a nearby hut. During the writing of this paper, flux measurements at the site continue uninterrupted, although fluxes recorded after 31 December 2015 will not be discussed in this paper.

The following meteorological measurements were recorded above the canopy: air temperature ( $T_a$ ) and relative humidity (RH) (model HMP45C, CSI), wind direction and speed (WS) (model 05103–10RE, R.M. Young), net radiation ( $R_n$ ) (model NR-LITE, Kipp and Zonen Ltd), downwelling and upwelling photosynthetically active radiation (PAR<sub>d</sub> and PAR<sub>u</sub>) (model Li–200S, LI-COR Inc.), and atmospheric pressure (model 61205V, R.M. Young Co.).  $T_a$  and RH were used to calculate vapour pressure deficit (VPD). Soil temperature ( $T_s$ ) was measured in profile at depths of 2, 5, 10, 20, 50, and 100 cm, using temperature probes (model 107B, CSI) at two locations. Soil moisture (VWC) was monitored by water content reflectometers (model 615, CS), which were buried at depths of 5, 10, 20, and 50 cm at the same two locations. Weighted average soil moisture content from 0–30 cm (VWC<sub>0–30cm</sub>) was computed to represent the root zone. Precipitation (P) was measured using an all-season heated tipping-bucket rain gauge (model 52202, R.M. Young) installed at a 1.5 m height. P measurements were cross checked and gap-filled with data from a weighted rain gauge (model T–200B, Geonor) placed in an open field from 2007 onwards at the Long Point Waterfowl Recreation and Education Centre. All meteorological and soil data were recorded at half hourly intervals using two data loggers (model CR10X/1000, CSI).

### **3.3 Data processing and gap-filling**

All flux and meteorological data was quality controlled and gap-filled following data collection by the Biometeorological Analysis, Collection, and Organizational Node (BACON) (Brodeur, 2014). Erroneous half-hourly meteorological data were removed using static thresholds, followed by more detailed visual scrutiny and manual removal.

### *3.3.1 Micrometeorological Data*

A number of different methods were employed to fill gaps in time series that are required to be continuous. For meteorological variables that were highly correlated between TPFS sites and measured concurrently (i.e.  $T_a$ , PARd, radiative fluxes, RH, WS, atmospheric pressure, and P), gaps in data from TP02 were filled by linear regression modeled values from a 76 year-old white pine forest (TP39; CA-TP4) from 2002–2012 and a newly established 80 year-old Carolinian forest (TPD; CA-TPD) from 2012 onwards. The source site used to fill gaps in target data was determined by the coefficient of determination ( $r^2$ ) for the given variable between sites for the year of interest. Data gaps were filled preferentially from the source site with highest  $r^2$ , where data was available. Any remaining gaps were filled from sites with the next highest  $r^2$  where data existed.

When filling gaps in meteorological variables that show poorer correlation across sites, a number of different approaches were used. Gaps in  $T_s$  measured at 2 cm and 5 cm depth were filled using a linear regression model based on  $T_a$  data. Gaps in top-30 cm averaged VWC ( $VWC_{0-30cm}$ ) were filled in a similar manner as methods described above for highly-correlated variables, except that an attempt was first made to fill data gaps for a given soil pit by a linear regression model with the other soil pit at TP02.  $R_n$  was filled using an artificial neural network (ANN), created with the MATLAB neural network toolbox and conditioned with  $T_a$ , PARd, WS, and RH inputs.

### *3.3.2 Flux Data*

Half-hourly carbon flux ( $F_c$ ) data measured using the OPEC system were corrected for density fluctuations due to sensible heat and water vapour fluxes (Webb et al., 1980), as well as instrument heating effects (Burba et al., 2008). All half-hourly flux measurements were subjected to coordinate rotation (Tanner and Thurtell, 1969), as well as outlier removal using an automated detection algorithm method, similar to Papale et al. (2006). Net ecosystem exchange (NEE) was calculated as  $NEE = F_c + S_c$  where  $S_c$  is the rate of change in  $CO_2$  storage within the air column below the EC sensor and  $F_c$  is the EC flux of  $CO_2$  (Fluxnet-Canada, 2003). Net ecosystem productivity (NEP) was calculated as  $NEP =$

- NEE, where a positive flux represents C fixed to the ecosystem (sink) and a negative flux represents C emitted to the atmosphere (source).

In order to improve confidence that measured NEE reflected the true ecosystem exchange, a friction velocity threshold ( $u_*^{Th}$ ) was applied to all nocturnal ( $PAR_d < 15 \mu\text{mol m}^{-2} \text{s}^{-1}$ ) NEE measurements, removing data from periods where  $\text{CO}_2$  transport by non-turbulent means (i.e. horizontal and vertical advection attributed to density flows and breezes) was non-negligible (Aubinet, 2008; Barr et al., 2013; Gu et al., 2005; Papale et al., 2006). Nocturnal half-hourly NEE values were removed when measured  $u_*$  was below thresholds estimated using the Moving Point Test  $u_*^{Th}$  determination method described by Papale et al. (2006), which estimated  $u_*^{Th}$  from the relationship between nighttime Net Ecosystem Exchange ( $NEE_n$ ) and  $u_*$ .

From 2008 to 2013, the CPEC flux data was subject to gap-filling using a modified version of the nonlinear estimation model used by Richardson et al. (2007) for the Howland Research Forest data (NLR-HL). The NLR-HL method calculates relationships separately for all years. Measured RE is assumed to be equal to NEE during nighttime and daytime when both  $T_a$  and  $T_s < 0^\circ\text{C}$  (i.e. when GEP is 0). RE is modelled as a function of  $T_s$  and  $VWC_{0-30\text{cm}}$  according to the relationship:

$$RE = R_{10} \times Q_{10}^{\frac{(T_s-10)}{10}} \times f(VWC_{0-30\text{cm}}), \quad (1)$$

where  $R_{10}$  and  $Q_{10}$  are fitted temperature response parameters that describe the relationship between RE and  $T_s$  (Brodeur, 2014).  $f(VWC_{0-30\text{cm}})$  is a sigmoidal function that characterizes the role of  $VWC_{0-30\text{cm}}$  in modifying the temperature response of RE as:

$$f(x) = \frac{1}{[1 + \exp(\theta_1 - \theta_2 x)]}, \quad (2)$$

$\theta_1$  and  $\theta_2$  are fitted parameters that allow this term to range between [0,1] as a function of the independent variable  $x$  (i.e.  $VWC_{0-30\text{cm}}$ ), thus acting as a scaling function on the  $T_s$ –

RE relationship. The scaling function was found to provide a statistically significant improvement to the performance of the RE model during period of low VWC (i.e. mid-summer) (Brodeur, 2014). On average, 91% of RE flux data from 2008 to 2013 was gap-filled.

GEP is estimated as RE – NEE and assumed to be zero during nighttime periods, and daytime half hours when  $T_a$  and  $T_s < 0$  (Brodeur, 2014). GEP is modeled by adding additional controlling variables to the formula used in the Fluxnet-Canada Research Network (NLR-FC) method described by Barr et al. (2004):

$$GEP = \frac{\alpha PARd A_{max}}{\alpha PARd + A_{max}} \times f(T_s) \times f(VPD) \times f(VWC_{0-30cm}). \quad (3)$$

The first term in eq. 2 defines a Michaelis-Menten relationship between PARd and GEP, where  $\alpha$  is the quantum yield (i.e. photosynthetic flux per quanta of PARd) and  $A_{max}$  is the photosynthetic capacity (i.e. light-saturated rate of CO<sub>2</sub> fixation). The second through fourth terms describe sigmoidal-type [0,1] scaling responses of GEP to  $T_s$ , VPD, and  $VWC_{0-30cm}$ , respectively (Brodeur, 2014). In turn, modeled GEP and modeled RE were used to fill gaps in NEE when instruments malfunctioned or atmospheric conditions violate the assumptions of the EC technique.

In previous studies at TPFS, OPEC flux data was filled with a model similar to NLR-HL, however RE and GEP data were pooled together from 2003 to 2007 to develop the relationships with environmental variables (Peichl et al., 2010c). Recently, Brodeur (2014) found this method to be invalid, as the potential for bias error to be introduced was very large. Thus, we no longer gap-fill OPEC NEE data with this method, since gap-filled OPEC fluxes were mostly synthetic and potentially introduced artificial trends (Brodeur, 2014).

Fluxes of H and LE were filled using artificial neural networks created with the MATLAB neural network toolbox (Brodeur, 2014). LE was modeled and filled using  $R_n$ ,

$T_{s5cm}$ , WS,  $VWC_{0-30cm}$ , and VPD as training and modelling variables. Similarly, H was modeled and filled using PARd, Rn, filled LE, and  $T_a$  as training and modelling variables. Following Amiro et al. (2006), either windowed linear regression or windowed mean diurnal variation approaches were used to fill any remaining gaps in LE or H (Brodeur, 2014).

A linear relationship between half-hourly, gap-filled measurements of turbulent ( $H + LE$ ) and radiative ( $Rn - G$ ) fluxes during the study period of 2003–2015 had a slope of 0.71, an intercept of  $7.51 \text{ Wm}^{-2}$  and a correlation coefficient  $r^2 = 0.93$  (**Figure 3**). This suggested that estimates of turbulent fluxes of H and LE were underestimated and/or that available energy was overestimated at values above zero. Non-closure of energy balance is common in applications of EC methods above forest ecosystems (Restrepo and Arain, 2005; Wilson et al., 2002). Corrections to NEP, due to lack of energy balance closure, were not applied due to the relatively flat terrain of TP02, in which horizontal and vertical advection was assumed to average to zero over long periods.

### 3.4 Biometric Measurements

Ongoing biometric measurements were measured at three permanent plots within TP02 since 2004, following the National Forest Inventory (NFI) guidelines (Canadian Forest Inventory Committee, 2008). Measurements were made at the end of each growing season. Tree height was measured using a Suunto clinometer. Diameter at tree base (Dbase) was measured from 2004 to 2009 and diameter at breast height (DBH) was measured from 2008 to 2013. Tree basal area ( $\text{m}^2$ ) was calculated with the following equation:

$$\text{Tree basal area} = \frac{\pi \cdot (DBH \text{ or } Dbase)}{40000} \quad (4)$$

Stand basal area (BA) was calculated as the product of tree basal area and stem density. Stand stem volume (V) was calculated from BA and mean tree height (H) using the standard biometric equation (Cannell, 1984):

$$V = f \cdot BA \cdot H \quad (5)$$

which includes a standard stem form factor (f) of 0.5 (Cannell, 1984). Further information regarding biometric studies conducted at TP02 can be found in Peichl and Arain (2006), Peichl et al. (2010c), and Kula (2013).

### 3.5 Canopy Leaf Area Index

Leaf area index (LAI) is defined as half of the total green leaf area, from all sides, per unit ground surface area (Chen et al., 2002). We used satellite-derived LAI data from Landsat 5 and Landsat 7 at the 30 m resolution, and included all the cloud-free images available from 2003 to 2013. LAI was calculated from a relationship with the Simple Ratio through an empirical model from Chen et al. (2002). The Simple ratio is calculated as  $\frac{\rho_{NIR}}{\rho_{red}}$ , the ratio between reflectances at the infrared ( $\rho_{NIR}$ ) and the red ( $\rho_R$ ) wavelengths (Jones and Vaughan, 2010). Furthermore, the LAI data derived from the satellite images are technically effective LAI since they do not contain corrections for clumping (Chen et al., 2002). Although Landsat 5 continued to operate until December 2012, the last cloud-free data measured from it was in 2011. LAI data was not available for 2012 due to cloudy conditions during satellite overpass. Successful cloud-free LAI measurements predominantly occurred during the growing season, as fluctuations in PARd suggest frequent cloudy conditions during spring and early summer months, which is characteristic of temperate regions.

### **3.6 Data Analysis**

We used the method described by Coursolle et al. (2012) to delineate the photosynthetic growing season. The growing season was identified using gap-filled GEP, due to the presence of large data gaps that were several weeks in length. We defined the onset of the growing season as the first occurrence of five consecutive days with a daily mean GEP exceeding 15% of the yearly daily maximum GEP. The offset of the growing season was defined as the first occurrence when the daily mean GEP fell below 15% of the maximum value for five consecutive days. To ensure each half-hourly data point was represented in the calculation of daily mean GEP, a 5-day moving average was used. All data management and data analysis was conducted in the MATLAB 8.3 software (MathWorks Inc., USA). Gap-filled data was used to compute annual and growing season values of meteorological variables, C fluxes, and water fluxes. Non gap-filled data was used for analysis in determining environmental controls on daily fluxes.

## CHAPTER 4: RESULTS

### 4.1 Stand Development and Growth

In 2002, the site was plowed and seedlings were planted (**Figure 4a**). Within the one year of planting, herbs and grasses grew rapidly and dominated the land and shaded out the small white pine seedlings (**Figure 4b**). Mowing between rows of planted trees was carried out in the initial 2-3 years in late summer, to suppress some of the vigorous growth of herbs and grasses and to allow the planted seedlings to establish themselves. Each year the small seedlings grew higher and accumulated more foliage, such that within 4 years, they began to dominate the landscape and overtook the herbaceous growth (**Figure 4c**). This growth was reflected in the biometric and LAI measurements at the site (**Figure 5a-c**). During the first 5 years since planting, annual LAI held constant around  $3 \text{ m}^2 \text{ m}^{-2}$ , after which it began to increase steadily (**Figure 5a**). By 2006, four years after planting, the seedlings reached the sapling stage, with the mean height reaching 2 m (**Figure 5b**). At this point, diameter at breast height (DBH) was developing (**Figure 5c**). We began measuring DBH in 2008, while diameter was measured at the base of juvenile trees (Dbase) prior to 2008. By 2013, the trees were approximately 6 m tall, with an estimated annual LAI of  $6.69 \text{ m}^2 \text{ m}^{-2}$ . The canopy was dense and closed, with pine trees dominating the forest cover, shading out all understory herbs and grasses (**Figure 4e,f**). **Table 2** lists stand characteristics with time. The growth and expansion of tree cover at the site with age affected the energy, carbon and water balances.

### 4.2 Energy Dynamics in the First Decade since Planting

The climate of the white pine forest was characterized by distinct seasonality alternating between warm summers and markedly cold winters. Meteorological variables from 1 January 2003 to 31 December 2015 are shown in **Figure 6**. A comparison of annual and growing season mean  $T_a$  and P over the study period to 30-year norms identified certain years as warm and dry (i.e. 2005), hot and wet (i.e. 2006 and 2011), hot and dry (i.e.

2007), hot (i.e. 2010 and 2012), wet (i.e. 2013 and 2014), and dry (i.e. 2015) (**Table 3**). The greatest impact of the expanding forest cover on the energy balance of the forest was in the decoupling of soil from the atmosphere. In the first few years, when the seedlings were small and vegetation cover was dominated by seasonal grasses and herbs, ground heat flux ( $G$ ) was positive, indicating a conduction of energy from the soil surface down into the subsurface (**Figure 7a**). However, around year 2009 (LAI of  $\sim 5$ , **Figure 5a**),  $G$  values decreased substantially and became negative in 2012. This is also reflected in the inter-annual variability of soil temperature ( $T_s$ ). Initially, the exposed sandy soil would receive direct heating from the sun and warm up substantially compared to air temperature ( $T_a$ ), such that the difference in  $T_a$  and  $T_{s20cm}$  was on average approximately  $3^\circ\text{C}$  (**Figure 8a**). However as the canopy developed and shaded the soil from direct sun exposure, this difference fell to approximately  $0.5^\circ\text{C}$ , reflecting that of a nearby mature 76 year-old planted white pine stand (TP39) (**Figure 8b**). In general,  $T_s$  experienced a slow decline throughout the study period, likely associated with shading from increased leaf area.

Although we did not measure shortwave radiation to compute surface albedo directly, we observed changes in total net radiation ( $R_n$ ) measured at TP02 during the first decade, which is indicative of surface albedo change with age. The effect of stand age on surface albedo was evident during the winter months (December to February). During the early stages of stand development, when the trees were small and the herbaceous vegetation died back in the winter, snow cover would dominate the site. Greater amounts of radiation were reflected by the bright surface, as shown with negative winter  $R_n$  values (**Figure 8a**). As the coniferous canopy developed and the surface became darker, more energy was absorbed and  $R_n$  became increasingly positive during winter. Mean monthly upwelling PAR ( $PAR_{up}$ ) show a decreasing trend over the years as the fractional absorption of photosynthetic radiative energy increased from greater leaf area (**Figure 8b**). Like  $R_n$ ,  $PAR_{up}$  was subject to winter peaks during periods of snow accumulation. However, monthly upwelling longwave radiation ( $L_{u}$ ) appeared relatively stable from

2005 to 2012 (**Figure 8c**). The emissivity of the growing stand was estimated using a linear relationship between bare soil (0.90) and closed canopy (0.98) values.

Latent (LE) and sensible (H) heat fluxes also reflected the structural changes and climatic conditions of the growing forest. We observed that summer LE flux increased with stand age (**Figure 9a**). In the initial years after planting, spring and fall fluxes did not differentiate much. Only when the seedlings grew into saplings around 2006, did spring LE have higher values than those of fall. While only summer LE fluxes increased with stand age, both spring and summer H fluxes increased with stand age (**Figure 9b**). In years that experienced unusually warm temperatures (i.e. 2005, 2007, and 2012), H peaked while LE fluxes were low, reflecting relatively dry conditions at the time.

#### **4.3 Carbon Dynamics in the First Decade since Planting**

NEP of our site went through large changes over the last decade. The carbon balance of our forest in the first decade since planting reflected both changing structure of the forest and site-scale meteorology. Annual NEP is unavailable for years 2003 to 2007, as the OPEC fluxes are only present in bi-weekly to monthly periods although inferences can still be made about the initial years of forest growth. In 2003, the periods during the latter half of the growing season were predominantly sources likely due to the low C uptake of seedlings and high respiration from the decomposition of mineral soil organic matter (**Figure 10c**). In 2004, the periods during the growing season were mostly sinks, owing to relatively high spring soil moisture and intense seasonal herbaceous growth. The intensity of weed growth almost fully covered the pine seedlings (**Figure 4b**). In 2005, the periods during the growing season were predominantly sources, owing to a spring dry spell that affected the onset of the growing season and subsequent summer heat stress (**Figure 10b**). This decrease in NEP due to climate was also observed at neighboring flux sites (i.e. TP39). In 2006 and 2007, the forest appears to have a productive growing season. The relatively constant fluxes in earlier years (2003–2007) may have been due to

the large gaps in data due to the use of roving OPEC system at the site, as biometric data shows a constant increase in the stature of vegetation. With the CPEC fluxes we can observe that at 5 years of age, TP02 is a consistent annual sink of C (**Figure 10a**). **Table 4** provides summary of annual and growing season C and ET fluxes. Since 2008, both annual GEP and RE fluxes increased substantially and continuously (**Figure 10a**). The rapid increase in both GEP and RE in later years was likely due to the expanding leaf area. Maximum daily GEP rates increased from approximately  $5 \mu\text{mol m}^{-2} \text{s}^{-1}$  in 2003 to  $24 \mu\text{mol m}^{-2} \text{s}^{-1}$  by 2015, causing the light response curve to have a large range (**Figure 11a, Table 5**). However, the LAI normalized light response curves are fairly similar throughout the years (**Figure 11b**).

The inter-annual variability of C fluxes have generally increased, as daily NEP fluxes have nearly doubled from  $-1.5 \text{ g C m}^{-2}$  to  $+1 \text{ g C m}^{-2}$  in 2003 to  $-4 \text{ g C m}^{-2}$  to  $+9.5 \text{ g C m}^{-2}$  in 2015 (**Figure 12**). As previously mentioned, the inter-annual variability of C fluxes measured by the OPEC system is relatively constant due to the presence of large gaps in data. C fluxes also experience greater monthly variation during the photosynthetic growing season, as opposed to the non-growing season. Typically NEP would peak in May, decrease sharply in July, and peak once more in August before decreasing towards the end of the growing season. The seasonal reduction in NEP was caused due to a decrease in GEP when constrained by meteorological conditions (e.g.  $T_a$ ,  $T_s$ , and VPD) while RE peaked. As a result, NEP exhibits a characteristic double peak in the summer, commonly observed at other age-sequenced stands at TPFS. Daily C fluxes depict the ecosystem as a C sink during the growing season and a C source predominantly during the non-growing season. The growing seasons of 2008 to 2013 can be observed from cumulative NEP, where the onset marks the rapid increase from the minimum NEP value and the offset occurs around the maximum NEP value (**Figure 13a**). The forest experienced an early onset during 2009, 2010, and 2012 whereas the latest onset and offset occurred in 2015.

#### 4.4 Water Dynamics in the First Decade since Planting

VWC was typically highest in winter and spring due the lack of root uptake during tree dormancy, in addition to snowmelt and heavy spring precipitation ( $\sim 0.15 \text{ m}^3 \text{ m}^{-3}$ ). At this site, VWC declines with the onset of photosynthetic activity in spring. VWC reaches a minimum in July ( $\sim 0.07 \text{ m}^3 \text{ m}^{-3}$ ) that coincides with greater demand, as shown in peak PARd, VPD,  $T_a$ , and  $T_s$  values (**Figure 6**). VWC rises again through the autumn-winter months, when atmospheric and physiological demand decreases and precipitation is available to replenish soil water storage.

Soil water dynamics had an interesting effect on tree growth. In the initial years following planting, the tree roots were quite shallow and small. In 2004, (Peichl and Arain, 2007) observed only  $0.196 \pm 0.026 \text{ t ha}^{-1}$  of fine roots in the 0-15 cm soil layer and  $0.045 \pm 0.039 \text{ t ha}^{-1}$  in the 15-35 cm layer, while only  $0.023 \pm 0.039 \text{ t ha}^{-1}$  of small roots were found in the 0-15 cm layer at our site, with no root mass in deeper soil layers. In 2014, Skubel et al. (2015) reported  $3.623 \pm 1.566 \text{ t ha}^{-1}$  and  $0.857 \pm 0.530 \text{ t ha}^{-1}$  of fine roots in the 0-15 cm and 15-35 cm soil layers at TP02, respectively. In addition,  $1.490 \pm 0.877 \text{ t ha}^{-1}$  and  $2.671 \pm 1.873 \text{ t ha}^{-1}$  of small roots were found in the 0–15 cm and 15-35 cm soil layers at TP02. Evidently, the root system has developed substantially over the first decade following tree planting. Observing the VWC time series (**Figure 10b**) shows that during the first few years, the upper ( $\text{VWC}_{5\text{cm}}$ ) and lower ( $\text{VWC}_{50\text{cm}}$ ) soil moisture values fluctuated and were quite separated. From 2006 onwards, the VWC of both soil depths developed strong characteristics of annual drawdown from spring through summer and then an increase from fall through winter. Furthermore, the differences between  $\text{VWC}_{5\text{cm}}$  and  $\text{VWC}_{50\text{cm}}$  diminish, likely reflecting the control of the expanding root system on the soil water dynamics within the soil profile and shading from the increasing canopy.

The rise in ET from 330 mm annually in 2003 to 400 mm in 2015 is associated with the rise in NEP. During the growing season, maximum daily ET ( $2 \text{ to } 4 \text{ mm d}^{-1}$ ) typically occurred during July (**Figure 10d**). The inter-annual variability of ET gradually increased

with stand age (**Figure 12g,13b**). During years with  $T_a$  stress (i.e. 2012) and/or P limitation (i.e. 2005 and 2007), the forest would experience an ET reduction during June and the annual ET and variability was lower. Although the stand experienced high annual  $T_a$  and low annual P in 2010, the early onset to the growing season allowed annual ET to reach 429 mm.

The relationship between daily GEP and ET throughout the year indicates stand-level water-use efficiency (WUE) (**Figure 14, Table 5**). There is a large scatter in the relationship ( $r^2 = 0.09$  to  $0.80$ ), with the greatest scatter occurring during the early years which lacked data from the large gaps. From 2003 to 2007, mean daily sequestration of C was 0.28 to 0.61 g for every kg of water transpired. From 2008 to 2013, mean daily sequestration of C was 1.36 to 3.95 g for every kg of water transpired, with the exception of 11.31 g C kg<sup>-1</sup> H<sub>2</sub>O occurring in 2010. This was due to occasions during the summer where peaks in GEP were coupled with low ET. Although there was a significant discrepancy between WUE calculated from OPEC data and CPEC data, we still observed that WUE increased with stand age.

#### 4.5 Climatic Controls

To assess the multiple correlation of meteorological variables as well as ET, NEP, RE, and GEP, several principle component analyses (PCA) were run (**Figure 15**). Variables clustered together on the variables factor map were positively correlated whereas variables orthogonal to each other were not correlated. The temperature cluster ( $T_a$ ,  $T_{s5cm}$ ,  $T_{s20cm}$ , and  $T_{s50cm}$ ) and the soil moisture cluster ( $VWC_{5cm}$ ,  $VWC_{0-30cm}$ , and  $VWC_{50cm}$ ) are weakly negatively correlated. The atmospheric cluster (VPD, PAR<sub>d</sub>, and R<sub>n</sub>) has a strong positive correlation with temperature and a weak negative correlation with soil moisture. P was weakly positively correlated with soil moisture, weakly negatively correlated with atmospheric controls, and had no correlation with temperature. ET, NEP, RE, and GEP are highly positively correlated with the atmospheric controls, with ET having the highest

degree of correlation and GEP the lowest. The fluxes are also positively correlated with temperature, with ET having the highest degree of correlation and GEP having the least. RE had the strongest negative correlation with soil moisture, while NEP had the least.

Linear regression analyses were run to show the daily effect of meteorological controls C and ET fluxes from 2003 to 2015. The main effect plots illustrate the relative effect of a meteorological control on the dependent flux, compared to other meteorological controls (**Figure 16**). Collectively, the main effect of these controls influence the dependent flux. NEP was found to be most influenced by Rn,  $T_{s5cm}$ , and  $T_{s20cm}$  with a model fit of  $r^2 = 0.516$ . RE was found to be most influenced by Rn,  $T_{s5cm}$ , and  $T_{s20cm}$  with a model fit of  $r^2 = 0.6132$ . GEP was found to be most influenced by PARd, Rn,  $T_a$ ,  $T_{s5cm}$ , and  $T_{s20cm}$  with a model fit of  $r^2 = 0.4687$ . Finally, ET was found to be most influenced by Rn,  $T_{s5cm}$ , and  $T_{s5cm}$  with a model fit of  $r^2 = 0.6715$ .

**Figure 17** demonstrated that the linear regression analysis did not entirely explain the models. The NEP, RE, and ET models appear to be poor predictors of high values and values close to zero. The RE, GEP, and ET models generate negative values which do not make any physical sense. Additionally, the residuals exhibit seasonality and autocorrelation which indicates that an intrinsic trend needs to be removed from model inputs (**Figure 18**).

## CHAPTER 5: DISCUSSION

### 5.1 Stand Development and Growth

It is important to note that our flux measurement instruments changed from an OPEC to CPEC system in 2008. We observed an increase in the slope of Landsat-derived LAI from 2007 onwards, coinciding with an increase in GEP-derived  $A_{\max}$  in 2008 which suggests that leaf foliage increased. However, the increase in tree diameter and height were fairly linear. During the 13 year study period, quantum yield ( $\alpha$ , mol CO<sub>2</sub> mol<sup>-1</sup> photons) and photosynthetic capacity ( $A_{\max}$ ,  $\mu\text{mol m}^{-2} \text{s}^{-1}$ ) increased steadily as the size and density of the canopy increased. When the canopy was sparse from 2003 to 2007, photosynthesis was strongly curvilinear and saturated at a relatively low irradiance (Law et al., 2001). When canopy cover increased from 2008 to 2015, the linearity of the photosynthetic light curve increased. This was due to a larger fraction of leaves shaded within the canopy that required greater irradiance to reach them (Law et al., 2001). Thus, this decrease in light-use efficiency occurs due to PARd saturation of the forest canopy (Arain and Restrepo-Coupe, 2005). Notable decreases in  $A_{\max}$  are observed in 2005 and 2012 likely due to water stress caused by summer dry spell and heat wave, respectively. Although heat stress and drought was observed in 2007, there was no detrimental effect to  $A_{\max}$ , but rather an increase in  $\alpha$ . As previously mentioned, we were unable to distinguish whether the increase in  $A_{\max}$  in 2008 was driven by instrumentation change or an increase in photosynthetic capacity by physiological means. However when evaluating the systems separately, LAI standardization revealed that changes in GEP response to PARd between years are related to increasing leaf area.  $\alpha$  and  $A_{\max}$  measured at this forest were comparable to those observed in other temperate forests. At TP02, the  $\alpha$  values were greater than those observed at a 6 year-old ponderosa pine stand (0.01) while  $A_{\max}$  values were similar (22.6) during a dry summer (Law et al., 2001). Krishnan et al. (2009) observed a 6 year-old Douglas-fir stand to have  $\alpha = 0.03$  and  $0.06$  and  $A_{\max} = 14.15$  and  $7.94$  during moist and dry conditions respectively. Their 18 year-old Douglas-fir stand was observed to have  $\alpha = 0.06$  and  $0.08$  and  $A_{\max} = 19.84$  and  $8.08$  during moist and dry

conditions respectively. Their large  $\alpha$  values relative to TP02 are due to the highly productive nature of their coastal forests in the Pacific Northwest. However, their high annual GEP is coupled with high RE (Krishnan et al., 2009).

## 5.2 Energy Dynamics in the First Decade since Planting

Over the past 20 years, studies have described energy fluxes on diurnal (Amiro, 2001; Baldocchi and Vogel, 1996), seasonal (Chen et al., 2004; McCaughey et al., 1997), and annual (Williams et al., 2014) time scales. The energy balance of forest ecosystems has been widely evaluated in literature (Amiro et al., 2006; Foken, 2008; Wilson et al., 2002). Here, we discuss the trends in energy fluxes in relation to the development of an afforested or planted site on a decadal time scale.

During the initial years (2003–2005), the seedlings were small and exposed to the atmosphere. Winter net radiation ( $R_n$ ) was negative during these years, likely owing to the lack of canopy cover as well as dieback of any surrounding grasses and herbs. This allowed snow cover to accumulate on the surface, subsequently increasing surface albedo and decreasing  $R_n$ . In 2006, winter  $R_n$  became positive likely due to the additive effect of significantly increased leaf area (3.65) and heavy P throughout the year, which decreased the surface albedo. In the monthly energy budget (not shown),  $R_n$  became positive in February and November for the first time. An increasing trend in  $R_n$  was observed as the canopy developed and decreased winter albedo furthermore. Likewise,  $PAR_{up}$  exhibits a decreasing trend with stand age which demonstrates the canopy's increased capacity to absorb  $PAR_{dn}$ . The winter snow-albedo effect can also be observed, but it dwindles as the stand progresses. Our use of  $R_n$  as an indicator of albedo is further supported by  $L_u$ , which is shown to be rather stable from 2005 to 2012 as decreasing  $T_{s5cm}$  is compensated by change in bare soil emissivity to close canopy emissivity. Only after several years of canopy closure does  $L_u$  decrease from lower  $T_{s5cm}$ .

Ground heat flux ( $G$ ) was positive (downwards) during spring and summer indicating movement of heat from the warmer soil surface to deeper layers, and the reverse process occurred in fall and winter.  $G$  followed the development of the coniferous canopy and peaked in 2007. The trend was mainly driven by the larger spring and summer  $G$  fluxes, although fall fluxes decreased negatively over time. Since  $T_s$  had been steadily declining over the years, the conduction of  $G$  fluxes from the subsurface to the soil surface may have offset cooling from canopy shading and subsequent snow accumulation. However in 2014 and 2015, spring and summer  $G$  fluxes begin to rise again. This may be due to decreasing  $T_{s5cm}$  finally influencing the radiation balance as previously mentioned.

Summer LE fluxes increased with age, with the exception of low values measured during the summer drought and heatwave of 2007 and 2012 respectively. Spring and fall LE fluxes did not differentiate until 2006, where increasing canopy cover allowed spring LE to have higher values. This is evident during 2010 and 2012, when spring LE was greater due to an earlier onset to the growing season. H fluxes increased with stand age in the spring and summer, owing to the increased transfer of heat from the surface to the atmosphere. H peaked during years that experienced high annual  $T_a$  (i.e. 2012) and growing season  $T_a$  (i.e. 2005, 2007, and 2011). Overall, the energy balance of our site in the 13 years since planting was largely dominated by the developing stand structure, however during extreme years climate also had an impact.

### **5.3 Carbon Dynamics in the First Decade since Planting**

The NEP of a new plantation forest is typically negative for several years after establishment as disturbance increases C losses by heterotrophic respiration ( $R_h$ ) and the NPP of the young trees is low (Lorenz and Lal, 2010). The period of net C loss via organic matter oxidation and mineralization may last between 5 and 15 years (Lorenz and Lal, 2010). Thus, the speed of stand recovery after disturbance or plantation is suggested to depend on the speed of GEP recovery against a background level of  $R_h$  (Giasson et al.,

2006). Once the canopy closes, NEP may stabilize for a number of years (Lorenz and Lal, 2010). However, any forest management practice that reduces the magnitude of  $R_h$  associated with the disturbance will propel the ecosystem to reaching a positive NEP quicker (Pregitzer and Euskirchen, 2004). TP02 was afforested on an abandoned agricultural field, containing low residual soil C resulting in significantly lower RE rates (Peichl et al., 2010a). It is this low soil C pool that allowed TP02 to have higher NEP rates and reach the C compensation point, when the forest switched from a C source to a C sink. Due to a lack of continuity in flux data to compute annual NEP for years 2003 to 2007, we are unclear of when TP02 becomes a consistent sink. However, we can decisively say that at 5 years of age, TP02 is a consistent annual sink of C. In contrast, the highly productive harvested Douglas-fir stands in British Columbia were estimated to reach the C compensation point in 18 years, due to the likelihood of higher soil C pools after harvest facilitating equally high RE (Coursolle et al., 2012). Bracho et al. (2012) reported similarly high rates of NEP and a C compensation point of 4 years in Florida slash pine plantations, established over previous plantations with stumps left in place. It is important to note however, that the stand was a strong C source with a 3-year mean of  $-550 \text{ g C m}^{-2}$  before becoming a C sink. Amiro et al. (2010) demonstrated that chronosequences across North America became C sinks within 10 to 20 years, regardless of disturbance type. Thornton et al. (2002) predicted needle-leaf forests to become sinks ranging from 4 years post-harvest to 16 years post-fire.

As leaf area develops, forest growth and the C stored in tree biomass increases (Lorenz and Lal, 2010). The assimilation of C in tree biomass eventually exceeds C loss from soil respiration. In young plantations, GEP is higher due to the planting of trees at higher densities (Arain and Restrepo-Coupe, 2005). High RE also occurs due to high tree density and thus high root biomass. Since plantations are even-aged stands, leaf area and fine roots are able to increase to fully occupy the canopy and root system (Lorenz and Lal, 2010). As previously mentioned, Peichl and Arain (2007) and Skubel et al. (2015) observed an increase in belowground root biomass with stand age at TPFS. Ultimately,

the net uptake of reforested plantations forests is greater than that of naturally grown forests (Arain and Restrepo-Coupe, 2005).

C uptake in temperate forests is largely influenced by historic land use (Caspersen et al., 2000). Harmon and Marks's (2002) simulation experiments indicated that the conversion of agricultural systems, which stored the least amount of landscape-level C, to forest systems had resulted in a net gain of C. We compared the NEP trajectory of TP02 with that of reforested young stands in North America in varying climate zones (**Figure 19a**; see **Supplementary Table 1** for more details). At 10 years, the NEP of TP02 was estimated to be  $183 \text{ g C m}^{-2} \text{ yr}^{-1}$  with a density of  $1567 \pm 29 \text{ trees ha}^{-1}$ . A naturally regenerating jack pine site in the southern boreal ( $12500 \pm 2458 \text{ trees ha}^{-1}$ ) was a weak sink ( $4 \text{ g C m}^{-2} \text{ yr}^{-1}$ ) at 10 years (Zha et al., 2009). TP02 was more productive than a 20-year old ponderosa pine site in Oregon with  $150 \text{ g C m}^{-2}$  (Vickers et al., 2012). However, the ponderosa site was planted at a density ( $260 \text{ trees ha}^{-1}$ ) lower than that found in plantation or naturally regenerating stands. When standardized with tree density, the ponderosa pine stand has a significantly greater NEP per tree compared to other sites, in which their relative standings with each other remain the same (**Figure 19b**). TP02 pales in comparison to slash pine plantations in sub-tropical Florida ( $2084 \pm 132 \text{ trees ha}^{-1}$ ;  $700 \text{ g C m}^{-2} \text{ yr}^{-1}$ ), although the plantations were initially strong carbon sources in the years following the clearcut (Bracho et al., 2012; Clark et al., 2004).

#### **5.4 Water Dynamics in the First Decade since Planting**

The WUE of our stand continually increased with age over the course of this study. GEP increased while water loss remained relatively constant, resulting in the gradual increase in observed WUE. Skubel et al. (2015) suggest that forest structure allowed the site to continue to grow while being conservative with water usage, thus maximizing WUE. During the initial years, the lack of canopy closure exposed the stomata to greater quantities of dry air creating a higher VPD. Additionally, evaporation was increased due to greater exposure of soils. This impact reduced as the canopy started closing the gap during later years. As LAI increases, transpiration may compensate for the loss of soil

evaporation. Young forests have shallow root systems that restricts movement of water which leaves them more vulnerable to water stress (Skubel et al., 2015). Jassal et al. (2009) observed higher peak ET at their 19 year-old and 7 year-old harvested Douglas-fir stands in the Pacific Northwest, due to transpiration from abundant deciduous understory and brush growth, respectively, during summer months. ET received greater contribution from the soil during other months (Jassal et al., 2009) When drastic declines in ET were observed at TP02 during drought events (i.e. 2007 and 2012), a corresponding peak in WUE was observed. The conservation of water during dry periods and continued growth resulted in a strong seasonal trend in WUE during these periods (not shown). Jassal et al. (2009) also observed seasonal variation in WUE in their 7-year-old stand. While their annual WUE varied with age from 0.5 to 4.1 g C m<sup>-2</sup> kg<sup>-1</sup>, TP02 was equally as variable ranging from 0.29 to 3.95 g C m<sup>-2</sup> kg<sup>-1</sup>. During the later years of development, our site's WUE exceeded that of a 25-year old naturally regenerating ponderosa pine stand (2.4 g C m<sup>-2</sup> kg<sup>-1</sup>) in semi-arid central Oregon (Irvine et al., 2004). Furthermore, Law et al. (2002) determined the WUE of 15 evergreen coniferous forests of different ages from the Fluxnet network to be 3.0 g C m<sup>-2</sup> kg<sup>-1</sup>.

Our annual ET values (330-429 mm) exceed and approach those of the 7-year old (239-322 mm) and 19-year old (362-454 mm) Douglas-fir stands respectively (Jassal et al., 2009). During drought-constrained years, annual ET values still exceeded those of a 20-year old drought-affected ponderosa pine stand (224 ± 36 mm and 269 ± 43 mm) in semi-arid central Oregon (Schwarz et al., 2004). From 2006 onwards, we noticed that VWC<sub>5cm</sub> and VWC<sub>50cm</sub> were very similar. It is possible that canopy development decoupled the topsoil from the atmosphere, as decreased exposure led to less drying and thus greater uniformity in moisture between the soil layers. In addition, the root system may have developed deep enough to tap deep soil water.

## 5.5 Interactions with Climate

Generally, seasonal variation in C fluxes at TP02 was attributed to the behavior of photosynthetic activity at the onset of the growing season and entrance into winter dormancy in autumn, as at other sites (Euskirchen et al., 2006). During the growing season, warm temperature and dry air masses induced a seasonal drawdown of VWC resulting in reductions in NEP during the summer months. Since 2008, we typically observed a pronounced double peak in NEP which is characteristic of other conifer forests in the area that experience soil water limitations during the summer (Arain and Restrepo-Couple, 2005). During the period of GEP decline, photorespiration may increase as it is used as a mechanism to dissipate excess heat at high irradiance levels (Lin et al., 2000). It is likely that reductions in GEP and NEP values were caused by decreasing soil water availability and increasing evaporative demand (Law et al., 2001). This decrease in VWC made it increasingly difficult for the roots to provide water to the trees and compensate for the simultaneous loss of water from the leaves. During severe drought stress, stomatal pores may close to decrease this demand, inhibiting photosynthesis (Lorenz and Lal, 2010). Sharp decreases in ET were subsequently observed during periods of seasonal drought. RE follows a similar trajectory to GEP, however it tends to peak shortly afterwards resulting in a moderate to severe decline in NEP depending on the severity of the seasonal summer drought. As the stand grew, the seasonal pattern in VWC became more pronounced, likely due to above and below ground moisture regulation by white pine trees.

Seasonal changes in Rn and PARd decreased atmospheric and physiological demand during August and September. Cooling reduced soil water stress and allowed stomata to open (Oke, 1987). The higher intake of CO<sub>2</sub> contributed to the second peak observed in NEP and hence ET. Foliar browning of older growth was observed on branches and their subsequent senescence occurred concurrently with a decrease in C fluxes. Similarly, transpiration was reduced by a decline in the number of stomatal openings from senescence, and the driving forces of evaporation (i.e. T<sub>a</sub>, T<sub>s</sub>, and VPD) were weaker.

During the winter, trees stopped sequestering carbon after entering dormancy and NEP was primarily influenced by RE. In Canada, the growing season is the longest in temperate forests that have higher annual precipitation (Brümmer et al., 2012). Our site had a longer growing season compared to stands of similar age in other regions of Canada because of its southern (latitude) location (Coursolle et al., 2012).

We found that our meteorological controls predicted 52%, 61%, 47%, and 67% of variability in daily NEP, RE, GEP, and ET fluxes respectively. Rn has one of the largest main effects on all fluxes, particularly because it is responsible for bringing energy into the forest ecosystem and its importance will keep increasing until the canopy stabilizes. GEP on the hand is also strongly influenced by PARd. Throughout the phenological development of the stand, for a given unit of PARd, progressively less was transmitted by the canopy as foliage expanded and LAI increased (Vose and Swank, 1990). Thus, increased amounts of PARd is required to penetrate to depths of leaf foliage within the canopy. Similar to Rn, the importance of PARd may continue to increase until the canopy stabilizes.

It is surprising that the main effect of VWC was quite low in affecting all fluxes. Decreased VWC<sub>0-30cm</sub> levels generally represented root uptake of H<sub>2</sub>O into the trees and subsequently higher ET fluxes. As stomata are one of the mechanisms controlling photosynthetic C gain, an increase in ET should result in increases in GEP and RE. Granier et al. (2007) reported that soil water stress induces stomatal regulation in forests when the relative extractable water of soils drops below a 0.4 threshold. Although they found NEP to decrease with increased water stress, it was to a lesser extent than GEP, due to the compensating effect of decreased Re (Granier et al., 2007). The reduction of soil respiration from water stress may in turn compensate for the effect of warmer temperatures (i.e. heat waves) (Ciais et al., 2005). Since this region is known to experience P and/or VWC limitations, perhaps these caveats have been incorporated into the seasonality of the site.

Lastly, the temperature cluster has a large main effect on all fluxes, especially  $T_{s5cm}$ ,  $T_{s20cm}$ , and  $T_a$  (GEP). This implies that future climate warming will have noticeable effects on C and ET fluxes. Of the two most frequent extreme events that affect forests in southern Ontario, heat waves will have a greater impact than drought, since P has a relatively low effect.

The results of our analysis on daily growing season variables compliment and add insight to previous studies. Krishnan et al. (2009) analyzed seasonal environmental variables to C fluxes for 6 year-old and 18 year-old Douglas-fir sites. Their seasonal aggregation of spring (MAM), summer (JJA), and autumn (SON) months corresponded to a typical growing season at TP02. At the 18 year-old site, NEP had significant ( $p < 0.05$ ) negative relationships with  $T_a$ ,  $T_s$ , and  $VWC_{0-30cm}$ , whereas GEP was negatively related to PARd, and VPD and RE were negatively related to  $T_a$  and  $T_s$ . At the 6-year old site, NEP had no significant relationships, whereas GEP and RE were significantly positively related to  $T_a$ . Although they did not test for relationships with  $R_n$ , our analysis is mostly in agreeance with theirs.

Coursolle et al. (2012) analyzed Fluxnet-Canada forests, including the TPFS chronosequences, over a 5-year period. For young sites, they determined by stepwise regression that annual GEP was 87% dictated by LAI and 3% by GSL. Coursolle et al. (2012) determined that snow (partial  $R^2 = 0.70$ ), LAI (partial  $R^2 = 0.13$ ),  $T_s$  (partial  $R^2 = 0.05$ ), and  $T_a$  (partial  $R^2 = 0.02$ ) explained 90% of variation in annual RE. However, they could not identify any significant regressions for annual NEP. Although we found strong positive correlation between LAI and annual C and ET fluxes (not shown), our sample size was limited. Additionally, leaf area may simply serve as a proxy for meteorological variables that contribute to optimal growth conditions.

## CHAPTER 6: CONCLUSION

This study reports eddy covariance fluxes of energy, C, and water in a 13 year-old afforested white pine stand (TP02) in southern Ontario, Canada, and investigates its meteorological controls. We conclude that:

- The inter-annual variability of C fluxes was strongly influenced by the effects of stand age (e.g. canopy development). The rapid increase in annual GEP and RE was likely due to increase leaf foliage (i.e. LAI) and increased biomass respiration (i.e. tree diameter and height). The relationship between GEP and PAR changed, with quantum yield and photosynthetic capacity increasing steadily as the canopy size increased.
- Energy fluxes of  $R_n$ ,  $G$ ,  $LE$ , and  $H$  were largely influenced by canopy development. The presence of canopy cover during the winter decreased albedo, increasing  $R_n$ . The decoupling of the soil and atmosphere was observed in  $T_s - T_a$  values, resulting in the gradual decrease in  $G$ . Summer  $LE$  fluxes increased with stand age, as well as spring and summer  $H$  fluxes. During years with extreme weather (e.g. 2005, 2007, 2012),  $H$  peaked while  $LE$  fluxes were low, demonstrating the influence of climate.
- The stand functioned as an annual C sink after 5 years of planting, and has continuously sequestered  $CO_2$  since. The low soil C stock from the site's history of agricultural use allowed the site to reach higher NEP rates earlier and reach the C compensation point much quicker than most temperate conifer forests in North America. Since 2008, the forest has sequestered a minimum of  $1188 \text{ g C m}^{-2}$  and daily rates ranged from  $-4 \text{ g C m}^{-2}$  to  $9 \text{ g C m}^{-2}$ . Daily C fluxes were influenced by climate, particularly during years with extreme weather.
- The root system has developed substantially over the first decade.  $VWC_{5\text{cm}}$  and  $VWC_{50\text{cm}}$  developed strong seasonal trends of annual drawdown through spring and summer and recharge through fall and winter. The two soil layers eventually aligned with each other.

- The inter-annual variability of ET gradually increased with stand age; however it is affected by extreme climate during the years of 2007, 2010, and 2012. Stand structure allowed the forest to continue to grow while being conservative with water usage, thus maximizing WUE. WUE has increased from 0.29 to 3.95 g C kg<sup>-1</sup> H<sub>2</sub>O from 2003 to 2015.

Our findings demonstrate the potential of white pine as a viable plantation species in southern Ontario, and in other regions in North America with similar site characteristics and climate to sequester atmospheric CO<sub>2</sub>. The knowledge gained from this research regarding the C sequestration in afforested stands will help in developing policies for better management of forest ecosystems in Canada.

## **CHAPTER 7: FUTURE WORKS**

Future work should aim to improve the models of C and ET fluxes. The comparison of observed values to fitted values suggests that linear regressions are not the best way to model explanatory variables. Rather, exponential models, especially ones that only predict positive values (in the case of RE, GEP, and ET) should be considered.

Evaluating the model residuals suggests that the input data should be subject to seasonal adjustment to remove the seasonal component from the time series. The resulting seasonally adjusted data will then be used to analyze random, non-seasonal trends as the forest develops. In addition, the model residuals demonstrate autocorrelation within input data. Although predictions from models with serially correlated data are considered unbiased, they usually have larger prediction intervals than necessary. Thus, autocorrelated meteorological and flux data should be accounted for.

## REFERENCES

- Abrams, M.D., 2001. Eastern White Pine Versatility in the Presettlement Forest: This eastern giant exhibited vast ecological breadth in the original forest but has been on the decline with subsequent land-use changes. *Bioscience* 51, 967–979.
- Amiro, B.D., 2001. Paired-tower measurements of carbon and energy fluxes following disturbance in the boreal forest. *Glob. Chang. Biol.* 7, 253–268.
- Amiro, B.D., Barr, A., Black, T., Iwashita, H., Kljun, N., Mccaughey, J., Morgenstern, K., Murayama, S., Nesic, Z., Orchansky, A., 2006. Carbon, energy and water fluxes at mature and disturbed forest sites, Saskatchewan, Canada. *Agric. For. Meteorol.* 136, 237–251.
- Amiro, B.D., Barr, A.G., Barr, J.G., Black, T.A., Bracho, R., Brown, M., Chen, J., Clark, K.L., Davis, K.J., Desai, A.R., Dore, S., Engel, V., Fuentes, J.D., Goldstein, A.H., Goulden, M.L., Kolb, T.E., Lavigne, M.B., Law, B.E., Margolis, H.A., Martin, T., Mccaughey, J.H., Misson, L., Montes-Helu, M., Noormets, A., Randerson, J.T., Starr, G., Xiao, J., 2010. Ecosystem carbon dioxide fluxes after disturbance in forests of North America. *J. Geophys. Res.* 115, G00K02.
- Arain, M.A., Restrepo-Coupe, N., 2005. Net ecosystem production in a temperate pine plantation in southeastern Canada. *Agric. For. Meteorol.* 128, 223–241.
- Aubinet, M., 2008. Eddy Covariance CO<sub>2</sub> flux measurement in nocturnal conditions: an analysis of the problem. *Ecol. Appl.* 18, 1368–1378.
- Bala, G., 2013. Digesting 400 ppm for global mean CO<sub>2</sub> concentration. *Curr. Sci.* 104, 1471–1472.
- Baldocchi, D., Falge, E., Gu, L., Olson, R., Hollinger, D., Running, S., Anthoni, P., Bernhofer, C., Davis, K., Evans, R., Fuentes, J., Goldstein, A., Katul, G., Law, B., Lee, X., Malhi, Y., Meyers, T., Munger, W., Oechel, W., Paw, K.T., Pilegaard, K., Schmid, H.P., Valentini, R., Verma, S., Vesala, T., Wilson, K., Wofsy, S., 2001. FLUXNET: A New Tool to Study the Temporal and Spatial Variability of Ecosystem–Scale Carbon Dioxide, Water Vapor, and Energy Flux Densities. *Bull. Am. Meteorol. Soc.* 82, 2415–2434.
- Baldocchi, D.D., 2003. Assessing the eddy covariance technique for evaluating carbon dioxide exchange rates of ecosystems: Past, present and future. *Glob. Chang. Biol.* 9, 479–492.
- Baldocchi, D.D., Vogel, C.A., 1996. Energy and CO<sub>2</sub> flux densities above and below a temperate broad-leaved forest and a boreal pine forest. *Tree Physiol.* 16, 5–16.
- Barr, A.G., Black, T.A., Hogg, E.H., Kljun, N., Morgenstern, K., Nesic, Z., 2004. Inter-annual variability in the leaf area index of a boreal aspen-hazelnut forest in relation to net ecosystem production. *Agric. For. Meteorol.* 126, 237–255.

- Barr, A.G., Richardson, A.D., Hollinger, D.Y., Papale, D., Arain, M.A., Black, T.A., Bohrer, G., Dragoni, D., Fischer, M.L., Gu, L., Law, B.E., Margolis, H.A., Mccaughey, J.H., Munger, J.W., Oechel, W., Schaeffer, K., 2013. Use of change-point detection for friction-velocity threshold evaluation in eddy-covariance studies. *Agric. For. Meteorol.* 171-172, 31–45.
- Boucher, J.-F., Bernier, P.Y., Munson, A.D., 2001. Radiation and soil temperature interactions on the growth and physiology of eastern white pine (*Pinus strobus* L.) seedlings. *Plant Soil* 236, 165–174.
- Bracho, R., Starr, G., Gholz, H.L., Martin, T.A., Cropper, W.P., Loescher, H.W., 2012. Controls on carbon dynamics by ecosystem structure and climate for southeastern U.S. slash pine plantations. *Ecol. Monogr.* 82, 101–128.
- Brodeur, J.J., 2014. Data-driven approaches for sustainable operation and defensible results in a long-term, multi-site ecosystem flux measurement program. McMaster University.
- Brümmer, C., Black, T.A., Jassal, R.S., Grant, N.J., Spittlehouse, D.L., Chen, B., Nestic, Z., Amiro, B.D., Arain, M.A., Barr, A.G., Bourque, C.P.-A., Coursolle, C., Dunn, A.L., Flanagan, L.B., Humphreys, E.R., Lafleur, P.M., Margolis, H.A., McCaughey, J.H., Wofsy, S.C., 2012. How climate and vegetation type influence evapotranspiration and water use efficiency in Canadian forest, peatland and grassland ecosystems. *Agric. For. Meteorol.* 153, 14–30.
- Burba, G., Anderson, D., 2010. A Brief Practical Guide to Eddy Covariance Flux Measurements: Principles and Workflow Examples for Scientific and Industrial Applications. LI-COR Biosciences.
- Burba, G.G., McDermitt, D.K., Grelle, A., Anderson, D.J., Xu, L., 2008. Addressing the influence of instrument surface heat exchange on the measurements of CO<sub>2</sub> flux from open-path gas analyzers. *Glob. Chang. Biol.* 14, 1854–1876.
- Canadian Forest Inventory Committee, 2008. Canada's National Forest Inventory ground sampling guidelines : specifications for ongoing measurement.
- Cannell, M.G.R., 1984. Woody biomass of forest stands. *For. Ecol. Manage.* 8, 299–312.
- Caspersen, J.P., Pacala, S.W., Jenkins, J.C., Hurtt, G.C., Moorcroft, P.R., Birdsey, R.A., 2000. Contributions of land-use history to carbon accumulation in U.S. forests. *Science* 290, 1148–1151.
- Chen, B., Black, T.A., Coops, N.C., Krishnan, P., Jassal, R., Brümmer, C., Nestic, Z., 2009. Seasonal controls on interannual variability in carbon dioxide exchange of a near-end-of rotation Douglas-fir stand in the Pacific Northwest, 1997-2006. *Glob. Chang. Biol.* 15, 1962–1981.
- Chen, J., Paw U, K.T., Ustin, S.L., Suchanek, T.H., Bond, B.J., Brosofske, K.D., Falk, M., 2004. Net Ecosystem Exchanges of Carbon, Water, and Energy in Young and

Old-growth Douglas-Fir Forests. *Ecosystems* 7, 534–544.

- Chen, J.M., Pavlic, G., Brown, L., Cihlar, J., Leblanc, S.G., White, H.P., Hall, R.J., Peddle, D.R., King, D.J., Trofymow, J.A., Swift, E., Van Der Sanden, J., Pellikka, P.K.E., 2002. Derivation and validation of Canada-wide coarse-resolution leaf area index maps using high-resolution satellite imagery and ground measurements. *Remote Sens. Environ.* 80, 165–184.
- Ciais, P., Reichstein, M., Viovy, N., Granier, a, Ogee, J., Allard, V., Aubinet, M., Buchmann, N., Bernhofer, C., Carrara, a, Chevallier, F., De Noblet, N., Friend, a D., Friedlingstein, P., Grünwald, T., Heinesch, B., Keronen, P., Knohl, a, Krinner, G., Loustau, D., Manca, G., Matteucci, G., Miglietta, F., Ourcival, J.M., Papale, D., Pilegaard, K., Rambal, S., Seufert, G., Soussana, J.F., Sanz, M.J., Schulze, E.D., Vesala, T., Valentini, R., 2005. Europe-wide reduction in primary productivity caused by the heat and drought in 2003. *Nature* 437, 529–533.
- Clark, K., Gholz, H., Castro, M., 2004. Carbon dynamics along a chronosequence of slash pine plantations in north Florida. *Ecol. Appl.* 14, 1154–1171.
- Coursolle, C., Margolis, H.A., Giasson, M.A., Bernier, P.Y., Amiro, B.D., Arain, M.A., Barr, A.G., Black, T.A., Goulden, M.L., McCaughey, J.H., Chen, J.M., Dunn, A.L., Grant, R.F., Lafleur, P.M., 2012. Influence of stand age on the magnitude and seasonality of carbon fluxes in Canadian forests. *Agric. For. Meteorol.* 165, 136–148.
- Dunn, A.L., Barford, C.C., Wofsy, S.C., Goulden, M.L., Daube, B.C., 2007. A long-term record of carbon exchange in a boreal black spruce forest: means, responses to interannual variability, and decadal trends. *Glob. Chang. Biol.* 13, 577–590.
- Euskirchen, E.S., Pregitzer, K.S., Chen, J., 2006. Carbon fluxes in a young, naturally regenerating jack pine ecosystem. *J. Geophys. Res.* 111, D01101.
- Fluxnet-Canada, 2003. Fluxnet-Canada Measurement Protocols.
- Foken, T., 2008. The energy balance closure problem: An overview. *Ecol. Appl.* 18, 1351–1367.
- Giasson, M.A., Coursolle, C., Margolis, H. a., 2006. Ecosystem-level CO<sub>2</sub> fluxes from a boreal cutover in eastern Canada before and after scarification. *Agric. For. Meteorol.* 140, 23–40.
- Goulden, M.L., Mcmillan, a M.S., Winston, G.C., Rocha, a V., Manies, K.L., Harden, J.W., Bond-Lamberty, B.P., 2011. Patterns of NPP, GPP, respiration, and NEP during boreal forest succession. *Glob. Chang. Biol.* 17, 855–871.
- Granier, A., Reichstein, M., Breda, N., Janssens, I.A., Falge, E., Ciais, P., Grünwald, T., Aubinet, M., Berbigier, P., Bernhofer, C., Buchmann, N., Facini, O., Grassi, G., Heinesch, B., Ilvesniemi, H., Keronen, P., Knohl, A., Kostner, B., Lagergren, F., Lindroth, A., Longdoz, B., Loustau, D., Mateus, J., Montagnani, L., Nys, C., Moors,

- E., Papale, D., Peiffer, M., Pilegaard, K., Pita, G., Pumpanen, J., Rambal, S., Rebmann, C., Rodrigues, A., Seufert, G., Tenhunen, J., Vesala, T., Wang, Q., 2007. Evidence for soil water control on carbon and water dynamics in European forests during the extremely dry year: 2003. *Agric. For. Meteorol.* 143, 123–145.
- Gu, L., Falge, E.M., Boden, T., Baldocchi, D.D., Black, T.A., Saleska, S.R., Suni, T., Verma, S.B., Vesala, T., Wofsy, S.C., Xu, L., 2005. Objective threshold determination for nighttime eddy flux filtering. *Agric. For. Meteorol.* 128, 179–197.
- Harmon, M.E., Marks, B., 2002. Effects of silvicultural practices on carbon stores in Douglas-fir – western hemlock forests in the Pacific Northwest, U.S.A.: results from a simulation model. *Can. J. For. Res.* 32, 863–877.
- IPCC, 2005. Carbon Dioxide Capture and Storage - Summary for Policy Makers. A Special Report of Working Group III of the Intergovernmental Panel on Climate Change. Cambridge, United Kingdom.
- IPCC, 2007. Climate Change 2007: The Physical Science Basis. Contribution of Working Group I to the Fourth Assessment Report of the Intergovernmental Panel on Climate Change, Cambridge University Press. Cambridge, United Kingdom and New York, NY, USA.
- IPCC, 2014. Climate Change 2014: Synthesis Report. Contribution of Working Groups I, II and III to the Fifth Assessment Report of the Intergovernmental Panel on Climate Change. Geneva, Switzerland.
- Irvine, J., Law, B.E., Kurpius, M.R., Anthoni, P.M., Moore, D., Schwarz, P. a, 2004. Age-related changes in ecosystem structure and function and effects on water and carbon exchange in ponderosa pine. *Tree Physiol.* 24, 753–63.
- Jarvis, P.G., Ibrom, A., Linder, S., 2005. Carbon forestry–Managing forests to conserve carbon, The carbon balance of forest biomes. Taylor & Francis, Oxon, UK.
- Jassal, R.S., Black, T.A., Spittlehouse, D.L., Brümmer, C., Nesic, Z., 2009. Evapotranspiration and water use efficiency in different-aged Pacific Northwest Douglas-fir stands. *Agric. For. Meteorol.* 149, 1168–1178.
- Johnson, E.A., Miyanishi, K., 2010. *Plant Disturbance Ecology: The Process and the Response*. Elsevier Science.
- Jones, H.G., Vaughan, R.A., 2010. *Remote sensing of vegetation: principles, techniques, and applications*. Oxford university press.
- Krishnan, P., Black, T.A., Jassal, R.S., Chen, B., Nesic, Z., 2009. Interannual variability of the carbon balance of three different-aged Douglas-fir stands in the Pacific Northwest. *J. Geophys. Res. Biogeosciences* 114, 1–18.
- Kula, M.V., 2013. *Biometric-Based Carbon Estimates and Environmental Controls within an Age-Sequence of Temperate Forests*. McMaster University.

- Law, B., Falge, E., Gu, L., Baldocchi, D., 2002. Environmental controls over carbon dioxide and water vapor exchange of terrestrial vegetation. *Agric. For. Meteorol.* 113, 97–120.
- Law, B.E., Goldstein, A.H., Anthoni, P.M., Unsworth, M.H., Panek, J.A., Bauer, M.R., Fracheboud, J.M., Hultman, N., 2001. Carbon dioxide and water vapor exchange by young and old ponderosa pine ecosystems during a dry summer. *Tree Physiol.* 21, 299–308.
- Lin, Z., Peng, C., Sun, Z., Lin, G., 2000. Effect of light intensity on partitioning of photosynthetic electron transport to photorespiration in four subtropical forest plants. *Sci. China. C. Life Sci.* 43, 347–354.
- Lorenz, K., Lal, R., 2010. *Carbon Sequestration in Forest Ecosystems*, Ecosystems. Springer.
- McCaughey, J.H., Lafleur, P.M., Joiner, D.W., Bartlett, P.A., Costello, A.M., Jelinski, D.E., Ryan, M.G., 1997. Magnitudes and seasonal patterns of energy, water, and carbon exchanges at a boreal young jack pine forest in the BOREAS northern study area. *J. Geophys. Res.* 102, 28997–29007.
- Oke, T.R., 1987. *Boundary layer climates*, 2nd ed. John Wiley & Sons, Ltd.
- Papale, D., Reichstein, M., Aubinet, M., Canfora, E., Bernhofer, C., Kutsch, W., Longdoz, B., Rambal, S., Valentini, R., Vesala, T., Yakir, D., 2006. Towards a standardized processing of Net Ecosystem Exchange measured with eddy covariance technique: algorithms and uncertainty estimation. *Biogeosciences* 3, 571–583.
- Parker, W.C., Elliott, K.A., Dey, D.C., Boysen, E., Newmaster, S.G., 2001. Managing succession in conifer plantations: converting young red pine (*Pinus resinosa* Ait.) plantations to native forest types by thinning and underplanting. *For. Chron.* 77, 721–734.
- Payeur-Poirier, J.L., Coursolle, C., Margolis, H. a., Giasson, M.A., 2012. CO<sub>2</sub> fluxes of a boreal black spruce chronosequence in eastern North America. *Agric. For. Meteorol.* 153, 94–105.
- Peichl, M., 2005. *Biomass and carbon allocation in white pine chronosequence*. McMaster University.
- Peichl, M., Arain, M.A., 2006. Above- and belowground ecosystem biomass and carbon pools in an age-sequence of temperate pine plantation forests. *Agric. For. Meteorol.* 140, 51–63.
- Peichl, M., Arain, M.A., 2007. Allometry and partitioning of above- and belowground tree biomass in an age-sequence of white pine forests. *For. Ecol. Manage.* 253, 68–80.
- Peichl, M., Arain, M.A., Brodeur, J.J., 2010a. Age effects on carbon fluxes in temperate

- pine forests. *Agric. For. Meteorol.* 150, 1090–1101.
- Peichl, M., Arain, M.A., Ullah, S., Moore, T.R., 2010b. Carbon dioxide, methane, and nitrous oxide exchanges in an age-sequence of temperate pine forests. *Glob. Chang. Biol.* 16, 2198–2212.
- Peichl, M., Brodeur, J.J., Khomik, M., Arain, M.A., 2010c. Biometric and eddy-covariance based estimates of carbon fluxes in an age-sequence of temperate pine forests. *Agric. For. Meteorol.* 150, 952–965.
- Pregitzer, K.S., Euskirchen, E.S., 2004. Carbon cycling and storage in world forests: Biome patterns related to forest age. *Glob. Chang. Biol.* 10, 2052–2077.
- Presant, E., Acton, C., 1984. The soils of the regional municipality of Haldimand-Norfolk. *Agric. Canada* 1, 100.
- Reichstein, M., Papale, D., Valentini, R., Aubinet, M., Bernhofer, C., Knohl, A., Laurila, T., Lindroth, A., Moors, E., Pilegaard, K., Seufert, G., 2007. Determinants of terrestrial ecosystem carbon balance inferred from European eddy covariance flux sites. *Geophys. Res. Lett.* 34, 1–5.
- Restrepo, N., Arain, M., 2005. Energy and water exchanges from a temperate pine plantation forest. *Hydrol. Process.* 49, 27–49.
- Schwalm, C.R., Black, T.A., Morgenstern, K., Humphreys, E.R., 2007. A method for deriving net primary productivity and component respiratory fluxes from tower-based eddy covariance data: a case study using a 17-year data record from a Douglas-fir chronosequence. *Glob. Chang. Biol.* 13, 370–385.
- Schwarz, P.A., Law, B.E., Williams, M., Irvine, J., Kurpius, M., Moore, D., 2004. Climatic versus biotic constraints on carbon and water fluxes in seasonally drought-affected ponderosa pine ecosystems. *Global Biogeochem. Cycles* 18, 1–17.
- Skubel, R., Arain, M.A., Peichl, M., Brodeur, J.J., Khomik, M., Thorne, R., Trant, J., Kula, M., 2015. Age effects on the water-use efficiency and water-use dynamics of temperate pine plantation forests. *Hydrol. Process.* 29, 4100–4113.
- Smith, A.M., Coupland, G., Dolan, L., Harberd, N., Jones, J., Martin, C., Sablowski, R., Amey, A., 2009. *Plant Biology*, 1st ed. Garland Science, New York.
- Thornton, P.E., Law, B.E., Gholz, H.L., Clark, K.L., Falge, E., Ellsworth, D.S., Goldstein, a. H., Monson, R.K., Hollinger, D., Falk, M., Chen, J., Sparks, J.P., 2002. Modeling and measuring the effects of disturbance history and climate on carbon and water budgets in evergreen needleleaf forests. *Agric. For. Meteorol.* 113, 185–222.
- United Nations, 2015. Adoption of the Paris Agreement. *Conf. Parties its twenty-first Sess.* 21932, 32.
- Vickers, D., Thomas, C.K., Pettijohn, C., Martin, J.G., Law, B.E., 2012. Five years of

- carbon fluxes and inherent water-use efficiency at two semi-arid pine forests with different disturbance histories. *Tellus, Ser. B Chem. Phys. Meteorol.* 64, 1–14.
- Vose, J.M., Swank, W.T., 1990. Assessing seasonal leaf area dynamics and vertical leaf area distribution in eastern white pine (*Pinus strobus* L.) with a portable light meter. *Tree Physiol.* 7, 125–134.
- Walker, L.R., Wardle, D. a., Bardgett, R.D., Clarkson, B.D., 2010. The use of chronosequences in studies of ecological succession and soil development. *J. Ecol.* 98, 725–736.
- Waring, R.H., Running, S.W., 2007. *Forest ecosystems: analysis at multiple scales*, 3rd ed. Elsevier.
- Webb, E.K., Pearman, G.I., Leuning, R., 1980. Correction of flux measurements for density effects due to heat and water vapour transfer. *Q. J. R. Meteorol. Soc.* 106, 85–100.
- West, P.W., 2014. *Growing plantation forests*, 2nd ed, Growing Plantation Forests. Springer International Publishing.
- Williams, C.A., Vanderhoof, M.K., Khomik, M., Ghimire, B., 2014. Post-clearcut dynamics of carbon, water and energy exchanges in a midlatitude temperate, deciduous broadleaf forest environment. *Glob. Chang. Biol.* 20, 992–1007.
- Wilson, K., Goldstein, A., Falge, E., Aubinet, M., Baldocchi, D., Berbigier, P., Bernhofer, C., Ceulemans, R., Dolman, H., Field, C., Grelle, A., Ibrom, A., Law, B., Kowalski, A., Meyers, T., Moncrieff, J., Monson, R., Oechel, W., Tenhunen, J., Valentini, R., Verma, S., 2002. Energy balance closure at FLUXNET sites. *Agric. For. Meteorol.* 113, 223–243.
- Zha, T., Barr, A.G., Black, T.A., McCaughey, J.H., Bhatti, J., Hawthorne, I., Krishnan, P., Kidston, J., Saigusa, N., Shashkov, A., Nesic, Z., 2009. Carbon sequestration in boreal jack pine stands following harvesting. *Glob. Chang. Biol.* 15, 1475–1487.

## TABLES

Table 1. Site characteristics.

|   |  |
|---|--|
| <b>Planting year</b>  | 2002 (seedling)  |
| <b>Location coordinates</b>                                   | 42.39' , 39.37" N<br>80.33' , 34.27" W   |
| <b>Elevation (m)</b>  | 265  |
| <b>Stand size (ha)</b>  | 10 with 5 ha conifer and 5 ha of deciduous stand on south and southwest.                         |
| <b>Dominant species</b>                                       | <i>Pinus strobus L.</i>  |
| <b>Ground Vegetation (as of 2013)</b>                         | Herbs, grasses ( <i>Digitaria sanguinalis</i> , <i>Trifolium repens</i> ,)                       |
| <b>Previous land use and management practices</b>             | Afforested on former agricultural land; fallow for 10 years prior to planting; stand not thinned |
| <b>Tree spacing (m x m)<sup>+</sup></b>                       | 2 x 2.5  |
| <b>Water table depth (m below surface)</b>                    | 2 - 3.5  |
| <b>Soil classification<sup>*</sup></b>                        | Brunisolic Gray Brown Luvisol  |
| <b>Soil texture<sup>*</sup></b>                               | 98% sand, 1% silt, <1% clay  |
| <b>Soil pH<sub>(CaCl)</sub> (0–10 cm)<sup>*</sup></b>         | 6.3  |
| <b>Bulk density (0–10 cm) (g cm<sup>-3</sup>)<sup>*</sup></b> | 1.49   |
| <b>Mineral soil C:N ratio (0–10 cm)<sup>*</sup></b>           | 11.4   |
| <b>Soil N (0–10 cm) (g m<sup>-2</sup>) / (%)<sup>*</sup></b>  | 86 / 0.06  |
| <b>Soil C (0–55 cm) (g m<sup>-2</sup>) / (%)<sup>*</sup></b>  | 3724 / 0.56  |
| <b>Mineral soil available P (ppm)<sup>a</sup></b>             | 169 ± 82   |
| <b>Mineral soil Mg (ppm)<sup>a</sup></b>                      | 44 ± 5   |
| <b>Mineral soil K (ppm)<sup>a</sup></b>                       | 48 ± 18  |
| <b>Mineral soil Ca (ppm)<sup>a</sup></b>                      | 1779 ± 753   |

<sup>+</sup> Reported by Peichl & Arain (2006)

<sup>\*</sup> Peichl et al. (2010), measured in 2007

<sup>a</sup> Khomik *et al.* (2010), top 20 cm measured in 2004

**Table 2.** Stand biometrics of TP02 (stand mean  $\pm$  within-stand standard deviation, na = not available).

| Values  | 2003 | 2004                              | 2005                              | 2006                              | 2007                              | 2008                              | 2009                              | 2010                              | 2011                              | 2012                              | 2013          | 2014                              |
|---|------|-----------------------------------|-----------------------------------|-----------------------------------|-----------------------------------|-----------------------------------|-----------------------------------|-----------------------------------|-----------------------------------|-----------------------------------|---------------|-----------------------------------|
| Mean Base Diameter (cm) <sup>a</sup>  | n/a  | 2.54 $\pm$ 0.75                   | 4.73 $\pm$ 1.13                   | 6.46 $\pm$ 1.34                   | 7.56 $\pm$ 1.5                    | 9.17 $\pm$ 1.81                   | 10.92 $\pm$ 1.97                  | n/a                               | n/a                               | n/a                               | n/a           | n/a                               |
| Mean DBH (cm) <sup>a</sup>  | n/a  | n/a                               | n/a                               | n/a                               | n/a                               | 5.34 $\pm$ 1.54                   | 7.00 $\pm$ 1.69                   | 8.33 $\pm$ 1.91                   | 10.45 $\pm$ 2.12                  | 11.63 $\pm$ 2.39                  | n/a           | 13.80 $\pm$ 2.72                  |
| Mean Tree Height (m) <sup>a</sup>   | n/a  | 0.95 $\pm$ 0.28                   | 1.37 $\pm$ 0.37                   | 2.01 $\pm$ 0.45                   | 2.83 $\pm$ 0.62                   | 3.57 $\pm$ 0.82                   | 3.81 $\pm$ 0.47                   | n/a                               | 5.07 $\pm$ 0.58                   | 5.79 $\pm$ 0.67                   | n/a           | n/a                               |
| Mean Tree Basal Area (m <sup>2</sup> ) <i>using base diameter</i>               | n/a  | 0.001 $\pm$ 2.15x10 <sup>-5</sup> | 0.002 $\pm$ 5.73x10 <sup>-5</sup> | 0.003 $\pm$ 9.11x10 <sup>-5</sup> | 0.005 $\pm$ 1.19x10 <sup>-4</sup> | 0.007 $\pm$ 1.19x10 <sup>-4</sup> | 0.010 $\pm$ 2.76x10 <sup>-4</sup> | n/a                               | n/a                               | n/a                               | n/a           | n/a                               |
| <i>using DBH</i>  | n/a  | n/a                               | n/a                               | n/a                               | n/a                               | 0.002 $\pm$ 8.97x10 <sup>-5</sup> | 0.004 $\pm$ 1.48x10 <sup>-4</sup> | 0.006 $\pm$ 2.15x10 <sup>-4</sup> | 0.009 $\pm$ 2.49x10 <sup>-4</sup> | 0.011 $\pm$ 3.06x10 <sup>-4</sup> | n/a           | 0.016 $\pm$ 5.65x10 <sup>-4</sup> |
| Stem Density (trees ha <sup>-1</sup> )  | n/a  | 1683 $\pm$ 147 <sup>b</sup>       | 1683 $\pm$ 147                    | 1683 $\pm$ 147                    | 1683 $\pm$ 189 <sup>c</sup>       | 1683 $\pm$ 189                    | 1683 $\pm$ 189                    | 1683 $\pm$ 189                    | 1683 $\pm$ 189                    | 1567 $\pm$ 29 <sup>d</sup>        | 1567 $\pm$ 29 | 1567 $\pm$ 29                     |
| Leaf area index (m <sup>2</sup> m <sup>-2</sup> )                               | 2.64 | 2.64                              | 2.91                              | 3.65                              | 3.43                              | 4.4                               | 5.08                              | 5.7                               | 6.4                               | n/a                               | 6.69          | n/a                               |
| Stand Basal Area (m <sup>2</sup> ha <sup>-1</sup> ) <i>using base diameter</i>  | n/a  | n/a                               | n/a                               | n/a                               | n/a                               | 11.54                             | 16.27                             | n/a                               | n/a                               | n/a                               | n/a           | n/a                               |
| <i>using DBH</i>  | n/a  | n/a                               | n/a                               | n/a                               | n/a                               | 4.08                              | 6.85                              | 9.65                              | 15.04                             | 17.33                             | n/a           | 25.07                             |
| Stand Stem Volume (m <sup>3</sup> ha <sup>-1</sup> ) <i>using base diameter</i> | n/a  | 0.45 $\pm$ 0.22 <sup>b</sup>      | 2.14                              | 5.78                              | 11.15                             | 20.62                             | 31.01                             | n/a                               | n/a                               | n/a                               | n/a           | n/a                               |
| <i>using DBH</i>  | n/a  | n/a                               | n/a                               | n/a                               | n/a                               | 7.29                              | 13.06                             | n/a                               | 38.15                             | 50.1 <sup>d</sup>                 | n/a           | n/a                               |

<sup>a</sup> Data from NFI (National Forest Inventory) plots monitored at TPFS forest stands from 2004

<sup>b</sup> Measured by Peichl & Arain (2006)

<sup>c</sup> Measured by Peichl et al. (2010)

<sup>d</sup> As of 2012, following (Kula, 2013); stem density includes trees  $\geq$  9 cm DBH

**Table 3.** Summary of annual (A) and growing season (GS) meteorological variables.

| Year                               | Mean Ta (°C)            |                          | Mean TS <sub>5cm</sub> (°C) |      | Mean Rn (W m <sup>-2</sup> ) |     | Mean PAR (µm m <sup>-2</sup> s <sup>-1</sup> ) |     | Mean VPD (kPa) |      | Mean VWC <sub>0-30cm</sub> (m <sup>3</sup> m <sup>-3</sup> ) |      | Total P (mm) |            | Growing Season Length    |
|------------------------------------|-------------------------|--------------------------|-----------------------------|------|------------------------------|-----|--|-----|----------------|------|--|------|--------------|------------|--------------------------|
|                                    | A                       | GS                       | A                           | GS   | A                            | GS  | A  | GS  | A              | GS   | A  | GS   | A            | GS         |                          |
| <b>2003</b>                        | 8.0                     | <i>14.1</i> <sup>a</sup> | 10.9                        | 17.2 | 55                           | 86  | 319  | 403 | 0.31           | 0.43 | 0.12   | 0.12 | <i>913</i>   | <i>607</i> | 227(85-312) <sup>c</sup> |
| <b>2004</b>                        | 8.4                     | 14.5                     | 11.8                        | 18.1 | 56                           | 88  | 316  | 403 | 0.30           | 0.41 | 0.10   | 0.12 | 956          | 549        | 230(87-317)              |
| <b>2005</b>                        | 8.7                     | <i>15.5</i>              | 12.4                        | 19.1 | 63                           | 98  | 351  | 444 | 0.35           | 0.50 | 0.05   | 0.05 | 862          | 556        | 233(87-320)              |
| <b>2006</b>                        | <b>9.7</b> <sup>b</sup> | 14.7                     | 12.2                        | 18.0 | 62                           | 92  | 318  | 408 | 0.33           | 0.44 | 0.12   | 0.12 | <b>1485</b>  | <b>953</b> | 230(86-316)              |
| <b>2007</b>                        | <b>9.0</b>              | <i>15.6</i>              | 12.0                        | 18.7 | 70                           | 109 | 334  | 446 | 0.39           | 0.57 | 0.11   | 0.10 | <b>705</b>   | <b>449</b> | 223(86-309)              |
| <b>2008</b>                        | 8.6                     | 14.9                     | 10.7                        | 16.8 | 72                           | 105 | 337  | 434 | 0.38           | 0.53 | 0.11   | 0.11 | <i>1140</i>  | 615        | 230(92-322)              |
| <b>2009</b>                        | 8.3                     | <b>13.3</b>              | 10.8                        | 15.4 | 70                           | 95  | 337  | 410 | 0.35           | 0.45 | 0.11   | 0.11 | 995          | 655        | 252(77-329)              |
| <b>2010</b>                        | <b>9.2</b>              | 14.5                     | 11.2                        | 15.9 | 73                           | 100 | 346  | 425 | 0.39           | 0.51 | 0.11   | 0.11 | 896          | 697        | 253(74-327)              |
| <b>2011</b>                        | <b>9.1</b>              | 15.0                     | 10.6                        | 15.7 | 68                           | 95  | 332  | 409 | 0.36           | 0.49 | 0.12   | 0.11 | <b>1293</b>  | <b>811</b> | 238(94-332)              |
| <b>2012</b>                        | <b>10.2</b>             | 14.5                     | 10.7                        | 14.6 | 78                           | 107 | 368  | 461 | 0.43           | 0.56 | 0.11   | 0.10 | 1001         | 696        | 256(73-329)              |
| <b>2013</b>                        | 8.5                     | 14.8                     | 9.0                         | 14.3 | 83                           | 115 | 232  | 439 | 0.34           | 0.46 | 0.11   | 0.10 | <b>1266</b>  | <b>843</b> | 228(96-324)              |
| <b>2014</b>                        | 7.5                     | 14.8                     | 8.3                         | 13.5 | 80                           | 111 | 259  | 328 | 0.32           | 0.46 | 0.11   | 0.11 | <b>1429</b>  | 700        | 220(98-318)              |
| <b>2015</b>                        | 8.6                     | 14.6                     | 8.8                         | 13.1 | 85                           | 107 | 326  | 386 | 0.34           | 0.45 | 0.10   | 0.10 | <b>811</b>   | 599        | 245(101-346)             |
| <b>30-Year Normal</b> <sup>d</sup> | 8.0                     | 14.9                     |                             |      |                              |     |  |     |                |      |  |      | 1036         | 632        |                          |

<sup>a</sup> *Italicized* numbers represent values of percentage increase in T<sub>a</sub> (4-10%) and P (10-15%) with relative to the 30-year norm.

<sup>b</sup> **Bolded** numbers represent values of percentage increase in T<sub>a</sub> (>10%) and P (>15%) relative to the 30-year norm.

<sup>c</sup> Growing season length (onset – offset)

<sup>d</sup> Environment Canada norms from 1981 to 2010 at Delhi, ON. Annual value (growing season; DOY 91-305)

**Table 4.** Summary of annual (A) and growing season (GS) C and ET fluxes.

| Year        | Total GEP<br>(g C m <sup>-2</sup> ) |      | Total RE<br>(g C m <sup>-2</sup> ) |      | Total NEP<br>(g C m <sup>-2</sup> ) |     | Total ET<br>(mm) |     | Growing<br>Season<br>Length |
|-------------|-------------------------------------|------|------------------------------------|------|-------------------------------------|-----|------------------|-----|-----------------------------|
|             | A                                   | GS   | A                                  | GS   | A                                   | GS  | A                | GS  |                             |
| <b>2003</b> | n/a                                 | n/a  | n/a                                | n/a  | n/a                                 | n/a | 330              | 272 | 227(85-312)                 |
| <b>2004</b> | n/a                                 | n/a  | n/a                                | n/a  | n/a                                 | n/a | 359              | 327 | 230(87-317)                 |
| <b>2005</b> | n/a                                 | n/a  | n/a                                | n/a  | n/a                                 | n/a | 351              | 309 | 233(87-320)                 |
| <b>2006</b> | n/a                                 | n/a  | n/a                                | n/a  | n/a                                 | n/a | 364              | 302 | 230(86-316)                 |
| <b>2007</b> | n/a                                 | n/a  | n/a                                | n/a  | n/a                                 | n/a | 342              | 299 | 223(86-309)                 |
| <b>2008</b> | 976                                 | 968  | 784                                | 703  | 191                                 | 264 | 390              | 358 | 230(92-322)                 |
| <b>2009</b> | 1137                                | 1119 | 1034                               | 939  | 105                                 | 180 | 368              | 347 | 252(77-329)                 |
| <b>2010</b> | 1412                                | 1398 | 1241                               | 1160 | 173                                 | 239 | 429              | 406 | 253(74-327)                 |
| <b>2011</b> | 1462                                | 1422 | 1252                               | 1141 | 216                                 | 281 | 377              | 348 | 238(94-332)                 |
| <b>2012</b> | 1473                                | 1439 | 1297                               | 1183 | 183                                 | 256 | 367              | 342 | 256(73-329)                 |
| <b>2013</b> | 1571                                | 1545 | 1394                               | 1248 | 180                                 | 296 | 401              | 367 | 228(96-324)                 |
| <b>2014</b> | n/a                                 | n/a  | n/a                                | n/a  | n/a                                 | n/a | 368              | 330 | 220(98-318)                 |
| <b>2015</b> | 1913                                | 1881 | 1774                               | 1599 | 140                                 | 282 | 400              | 367 | 245(101-346)                |

**Table 5.** Water use efficiency (WUE; g C kg<sup>-1</sup> H<sub>2</sub>O) from the monthly GEP and ET relationship.  $\alpha$  and  $A_{\max}$  values for the rectangular hyperbolic curve ( $GEP = \frac{\alpha PAR A_{\max}}{\alpha PAR + A_{\max}}$ ) fitted onto the GEP and PARd relationship.  $\alpha$  is the quantum yield (i.e. photosynthetic flux per quanta of PAR; mol CO<sub>2</sub> mol<sup>-1</sup> photons) and  $A_{\max}$  is the photosynthetic capacity (i.e. light-saturated rate of CO<sub>2</sub> fixation;  $\mu$ -mol m<sup>-2</sup> s<sup>-1</sup>). Values computed by the modified NLR-HL method are reported in brackets. The goodness of fit of each regression is given by  $r^2$ .

| <b>Year</b> | <b>WUE</b> | <b>r<sup>2</sup></b> | <b><math>\alpha</math></b> | <b>A<sub>max</sub></b> | <b>r<sup>2</sup></b> |
|-------------|------------|----------------------|----------------------------|------------------------|----------------------|
| <b>2003</b> | 0.2864     | 0.5413               | 0.0185                     | 5.8566                 | 0.8649               |
| <b>2004</b> | 0.6127     | 0.2002               | 0.0172                     | 12.9907                | 0.9204               |
| <b>2005</b> | 0.371      | 0.2618               | 0.0322                     | 4.3657                 | 0.8418               |
| <b>2006</b> | 0.3509     | 0.5358               | 0.0223                     | 6.6702                 | 0.8984               |
| <b>2007</b> | 0.5026     | 0.087                | 0.0551                     | 6.5985                 | 0.9377               |
| <b>2008</b> | 1.355      | 0.7596               | 0.0206<br>(0.0478)         | 19.7968<br>(39.5968)   | 0.9958               |
| <b>2009</b> | 2.7632     | 0.7875               | 0.0277<br>(0.0522)         | 17.3741<br>(23.7995)   | 0.9905               |
| <b>2010</b> | 11.3081    | 0.5276               | 0.0306<br>(0.0903)         | 23.5612<br>(44.7878)   | 0.992                |
| <b>2011</b> | 3.4524     | 0.8037               | 0.0304<br>(0.1029)         | 28.1987<br>(85.7944)   | 0.9947               |
| <b>2012</b> | 3.8087     | 0.7968               | 0.0294<br>(0.0429)         | 23.5071<br>(37.7239)   | 0.9912               |
| <b>2013</b> | 3.0248     | 0.6653               | 0.0375<br>(0.1073)         | 27.2911<br>(83.2004)   | 0.9908               |
| <b>2014</b> | n/a        | n/a                  | n/a                        | n/a                    | n/a                  |
| <b>2015</b> | 3.9479     | 0.748                | 0.0451<br>(0.0730)         | 33.6391<br>(67.3699)   | 0.997                |

**FIGURES**

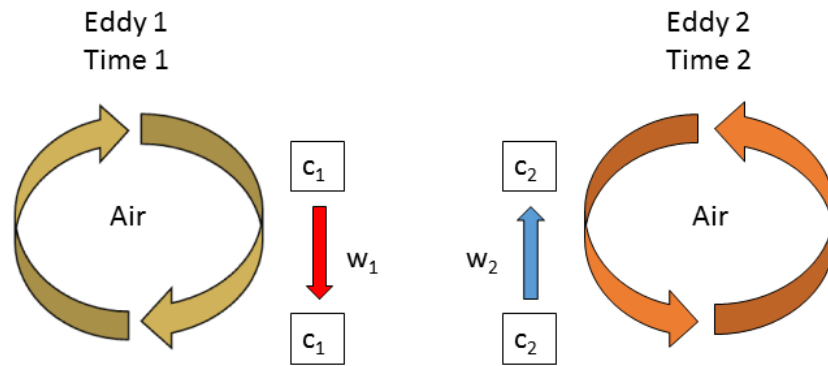


**Figure 1.** At a single point on the tower, eddy 1 moves air parcel with concentration  $c_1$  down with the vertical speed  $w_1$ , then eddy 2 moves air parcel with concentration  $c_2$  up with vertical speed  $w_2$ . Since each parcel has a concentration, temperature, humidity, and speed – the flux can be calculated (Burba and Anderson, 2010).

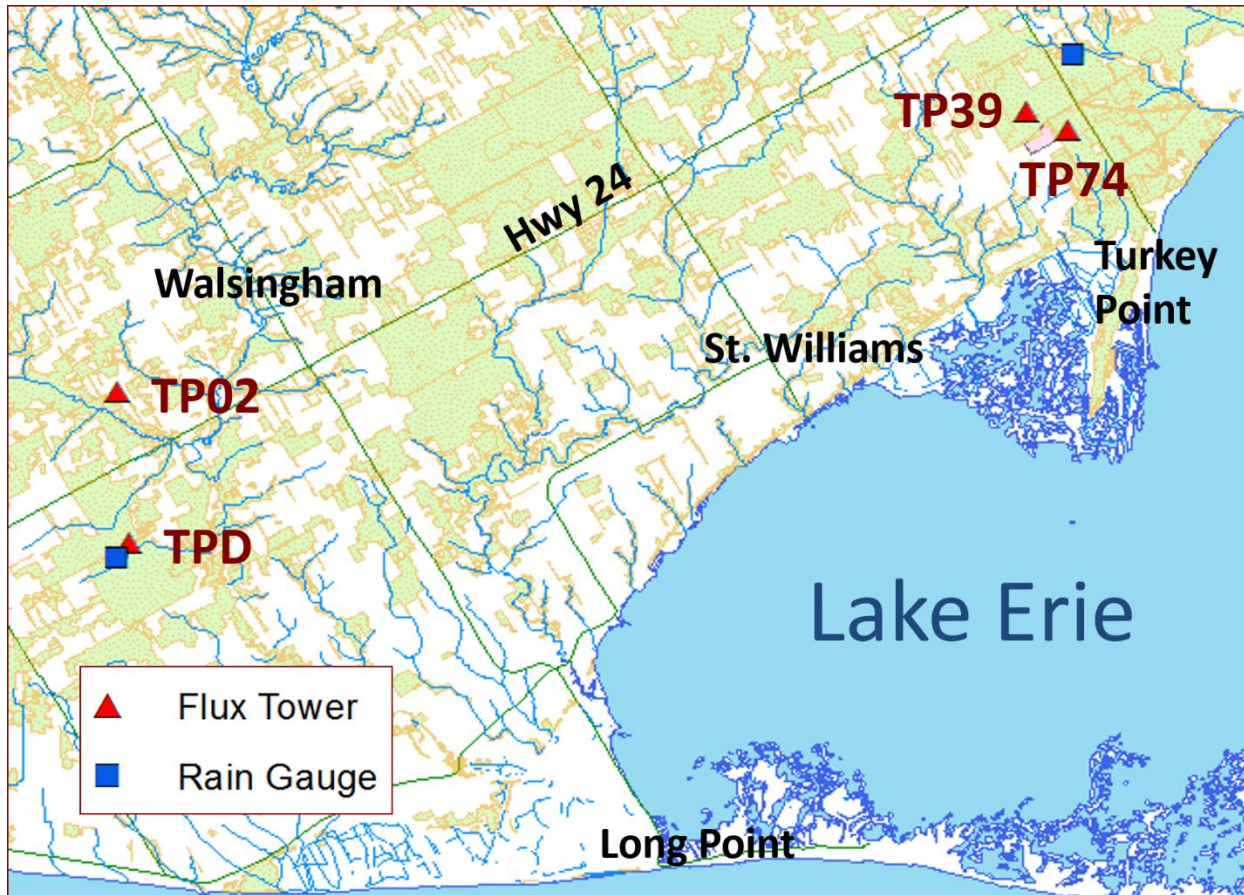


**Figure 2.** Location of four FLUXNET-associated tower sites in southern Ontario. White pine forests were planted in 1939 (TP39 or CA-TP4), 1974 (TP74 or CP-TP3, and 2002 (TP02 or CA-TP1). The deciduous forest site is naturally regenerating but managed site (TPD or CA-TPD).

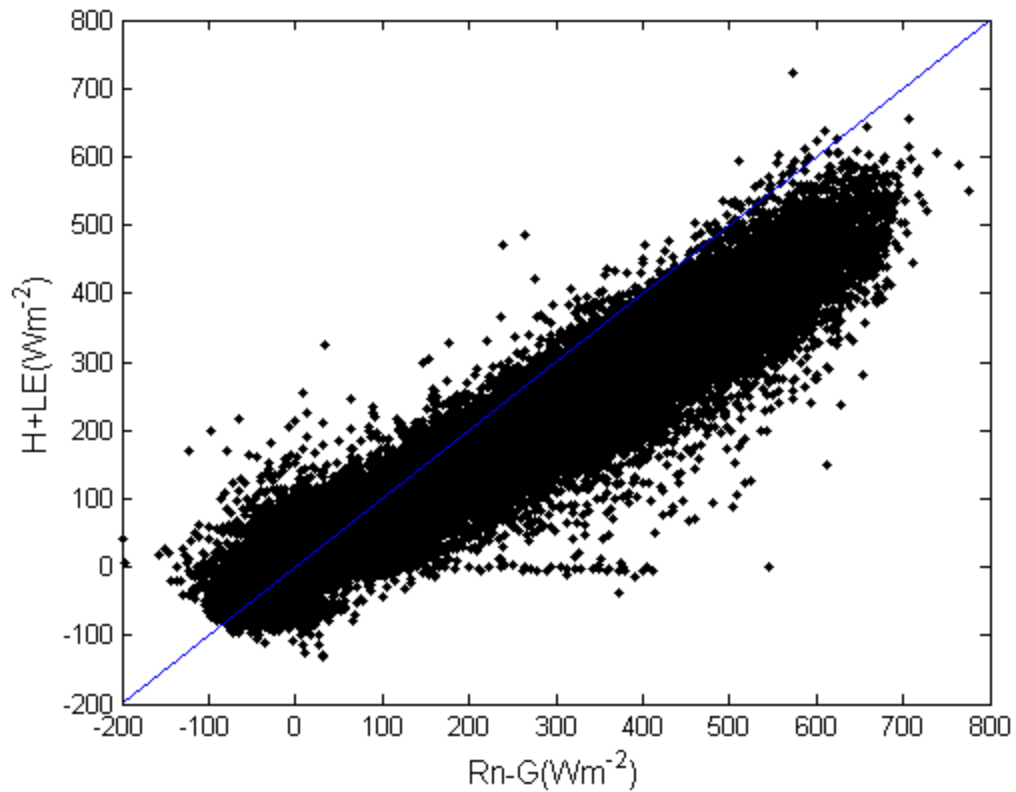


**Figure 3.** The half-hourly energy balance of the white pine forest plantation from 1 January 2003 to 31 December 2015. The sum of sensible heat flux H and latent heat flux LE is plotted against the sum of net radiation Rn and soil heat flux G. The slope of the regression line is 0.71 with an intercept of 7.51 W m<sup>-2</sup>. The adjusted correlation coefficient  $r^2$  is 0.93.



**Figure 4:** Progress of vegetation growth at TP02 over the past 11 years: (a) 2002 – seedlings planted, (b) 2003 – 1 year after planting, (c) 2006 – 4 years after planting, (d) 2009 – 7 years after planting, (e) 2011 – 9 years after planting, and (f) 2015 – 13 years after planting.

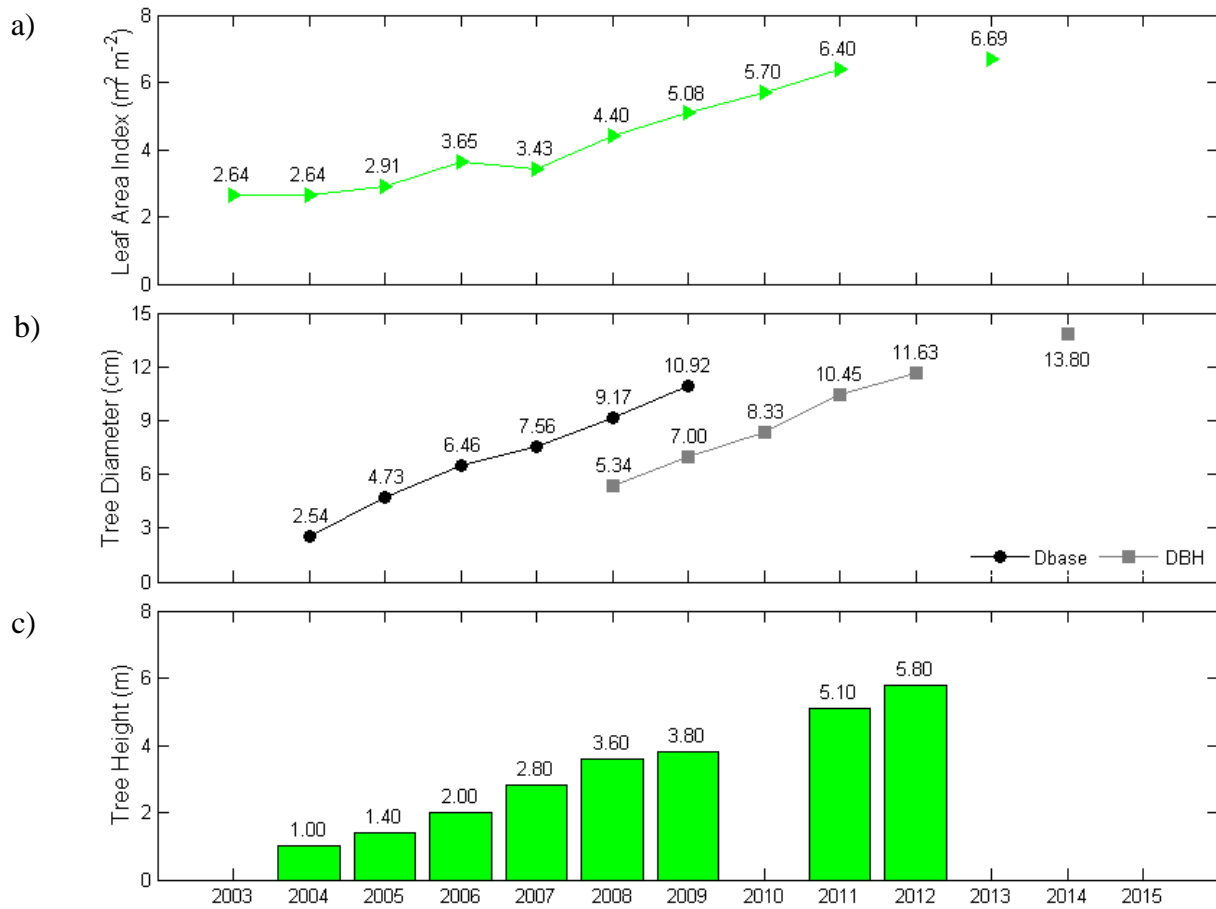


**Figure 5.** (a) Mean annual leaf area index (LAI) from Landsat 5 and Landsat 7 at the 30m resolution. Only cloud-free measurements were used. The correlation coefficient of annual LAI is 0.96. (b) Mean annual tree height. (c) Mean tree diameter at tree base (Dbase) and diameter at breast height (DBH) measurements from National Forest Inventory plots (NFI) within TP02.

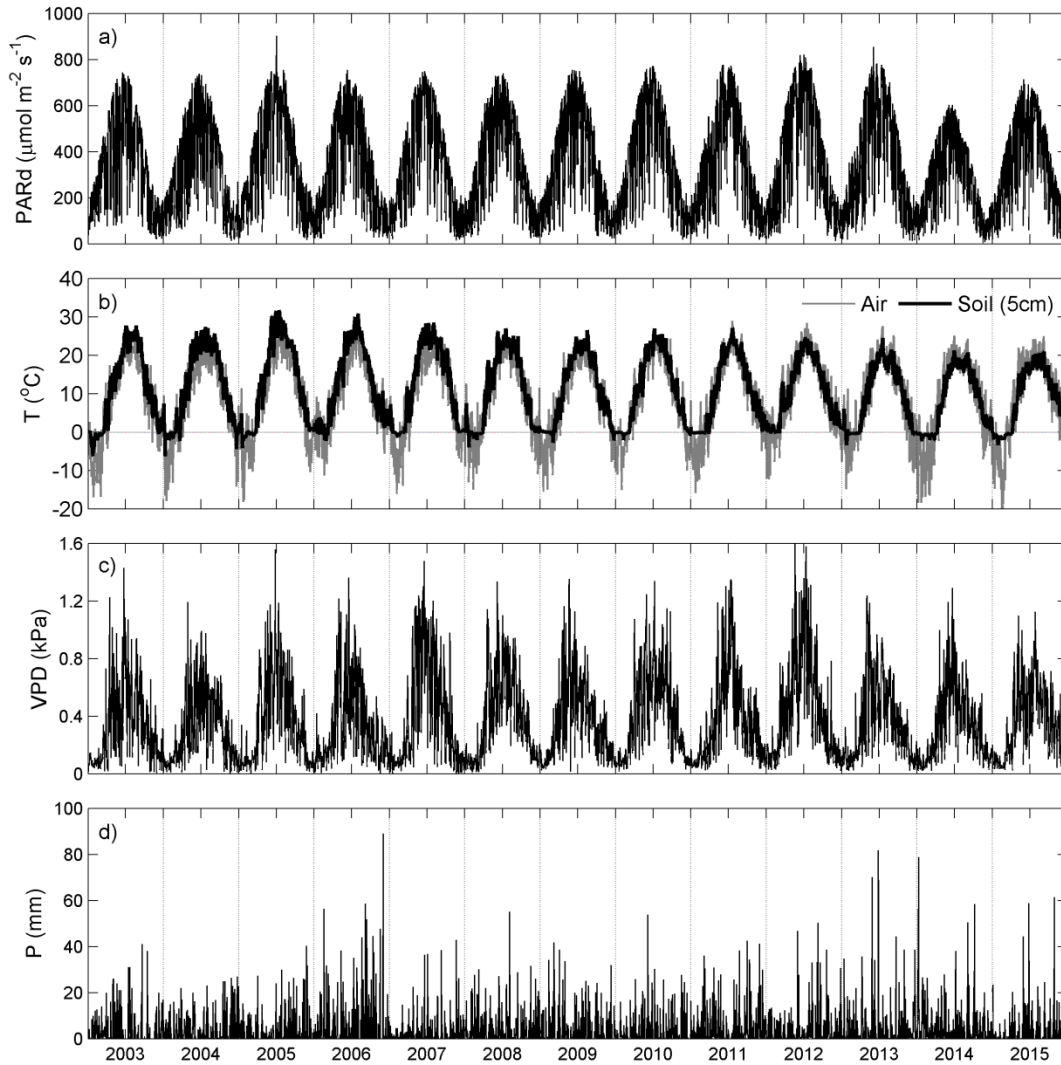


**Figure 6.** (a) Daily mean photosynthetically active radiation (PARd), (b) daily mean air temperature ( $T_a$ ) and daily mean soil temperature ( $T_s$ ) at 5 cm, (c) daily mean vapour pressure deficit (VPD), and (d) daily total precipitation (P) from 1 January 2003 to 31 December 2015. X axis tick marks indicate the beginning, mid, and end points of years.

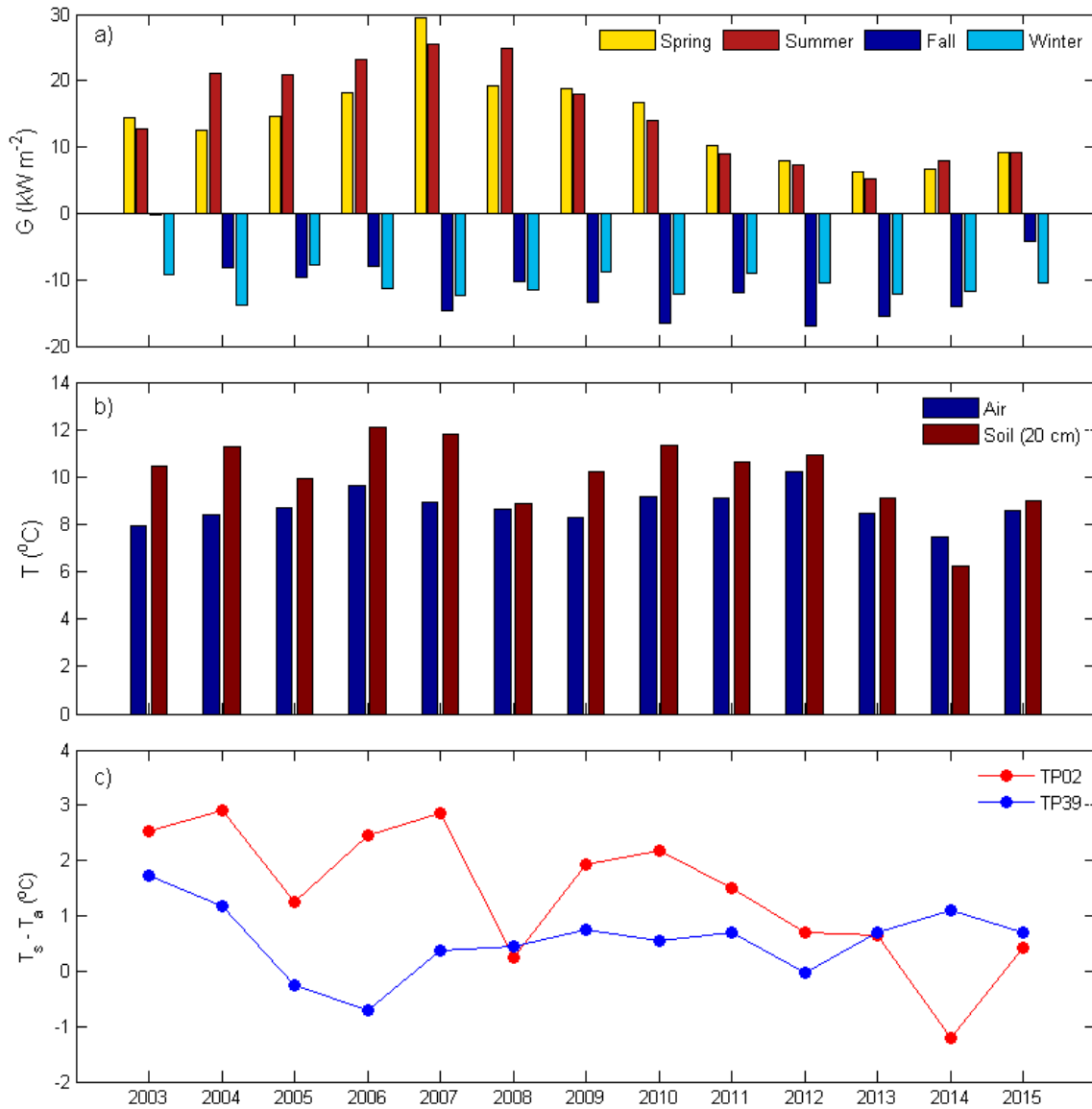


**Figure 7.** (a) Seasonal energy fluxes of ground heat flux ( $G$ ), (b) mean annual air ( $T_a$ ) and soil ( $T_{s20\text{cm}}$ ) temperature at 20 cm depth at TP02, and (c) the difference between mean annual  $T_a$  and  $T_{s20\text{cm}}$  at TP02 and TP39.

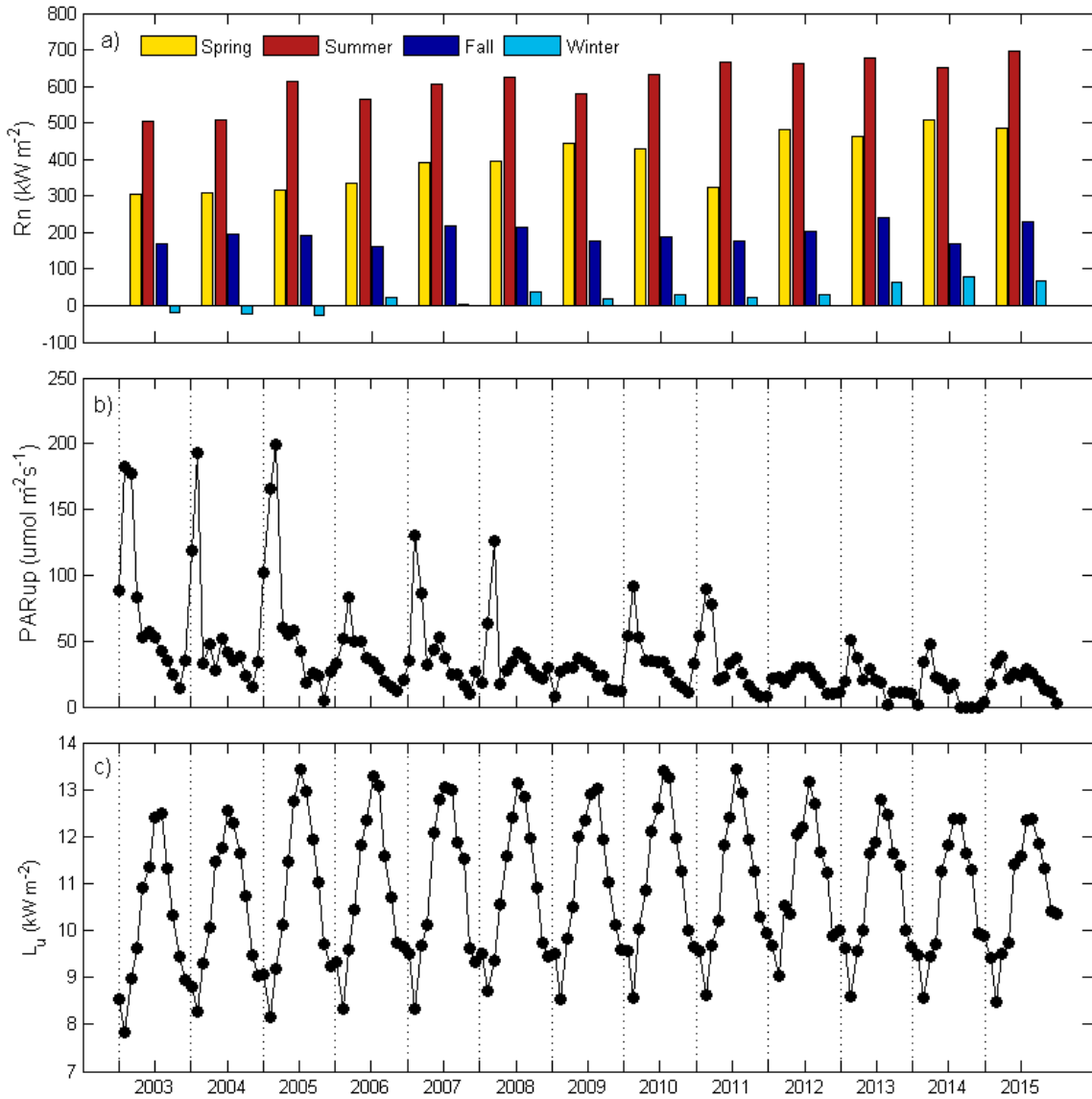


**Figure 8.** (a) Seasonal energy fluxes of net radiation ( $R_n$ ), (b) mean monthly upwelling PAR ( $\text{PAR}_{up}$ ), and (c) monthly upwelling longwave radiation ( $L_u$ ).

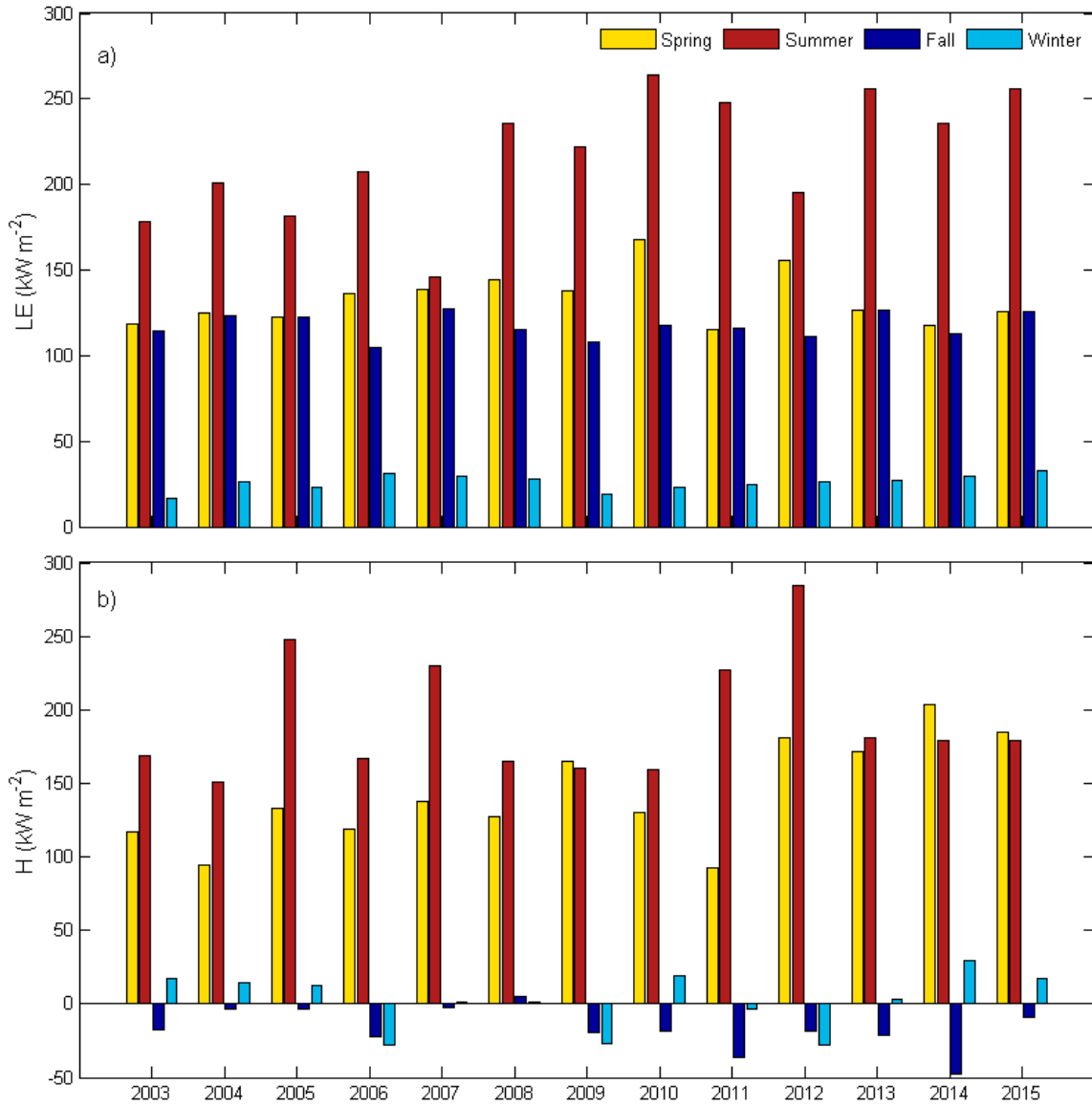


**Figure 9.** Seasonal energy fluxes of (a) latent heat (LE) and (b) sensible heat (H).

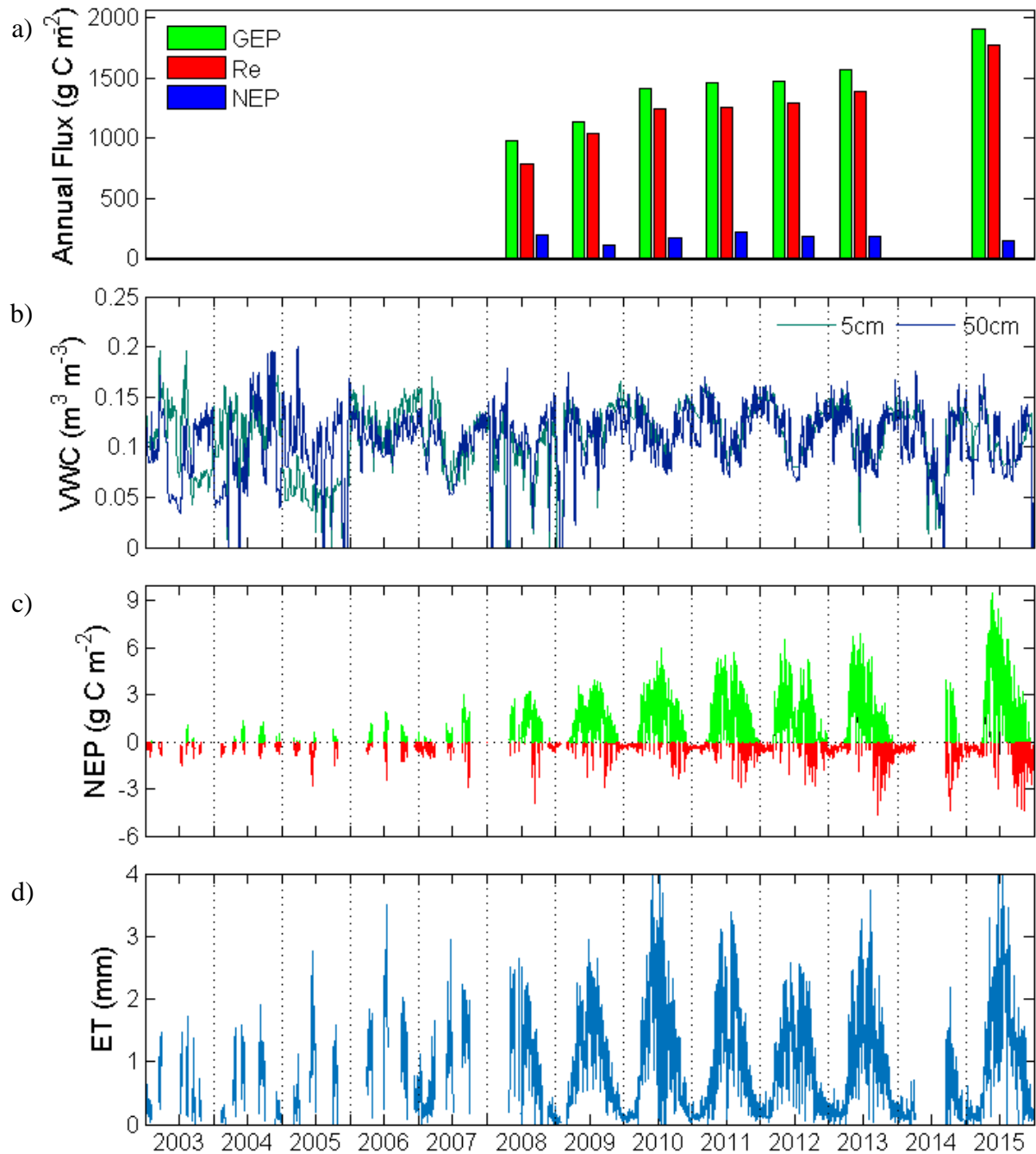


**Figure 10.** (a) Annual fluxes of gross ecosystem productivity (GEP), ecosystem respiration (RE), and net ecosystem productivity (NEP). (b) Daily mean volumetric water content at 5 cm (VWC<sub>5cm</sub>) and 50 cm (VWC<sub>50cm</sub>) soil depth, (c) NEP, and (d) evapotranspiration (ET) from 1 January 2003 to 31 December 2015.

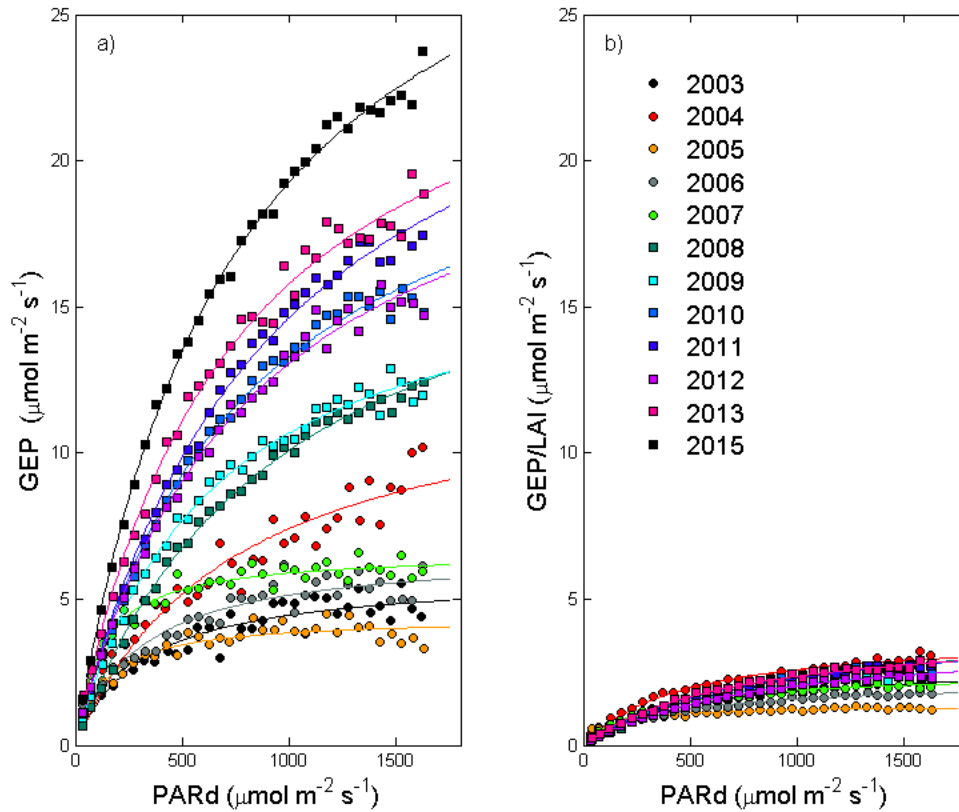


**Figure 11.** a) The rectangular hyperbolic curve ( $GEP = \frac{\alpha PARd A_{max}}{\alpha PARd + A_{max}}$ ) fitted to bin-averaged ( $10 \mu\text{mol m}^{-2}\text{s}^{-1}$ ), half-hourly data gross ecosystem productivity (GEP) and photosynthetically active radiation (PARd). GEP fluxes from 2014 were not fitted to this curve due to extensive gap-filling resulting from data loss during the growing season.  $\alpha$  ( $\text{mol CO}_2 \text{ mol}^{-1} \text{ photons}$ ) and  $A_{max}$  ( $\mu\text{mol m}^{-2} \text{ s}^{-1}$ ) values are derived from this relationship. The  $r^2$  goodness of fit for the regressions ranged from 0.84 to 0.99. b) Normalized curve with annual LAI. The GEP curve from 2015 was not standardized since LAI data was not available.

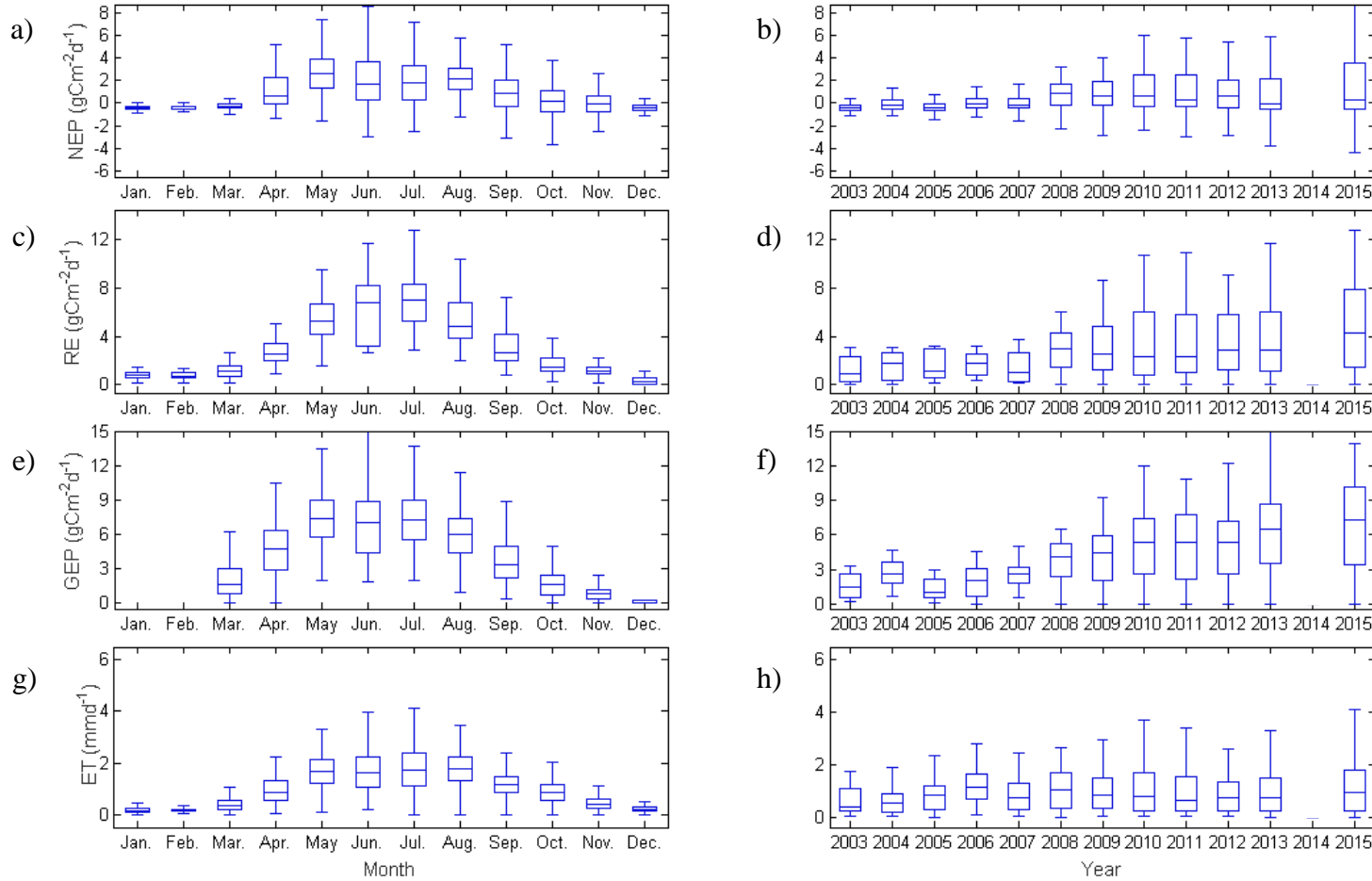


**Figure 12.** Monthly and annual box plots of daily fluxes of NEP, RE, GEP, and ET fluxes.

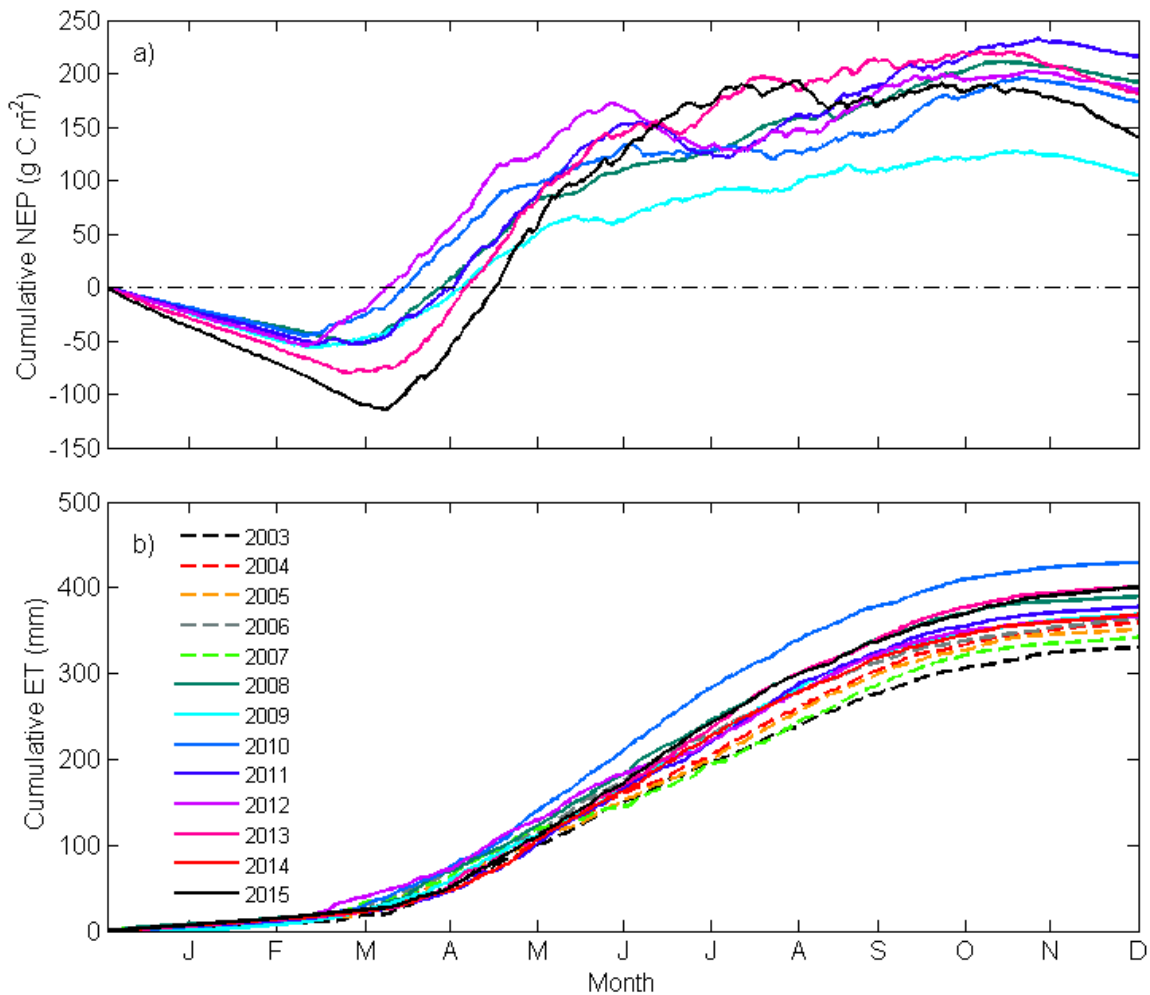


**Figure 13.** Monthly cumulative (a) NEP and (b) ET. Data measured with the OPEC system is represented by dashed lines while data measured by the CPEC system is represented by solid lines. Cumulative NEP from 2014 is not shown due to extensive gap-filling resulting from data loss during the growing season.

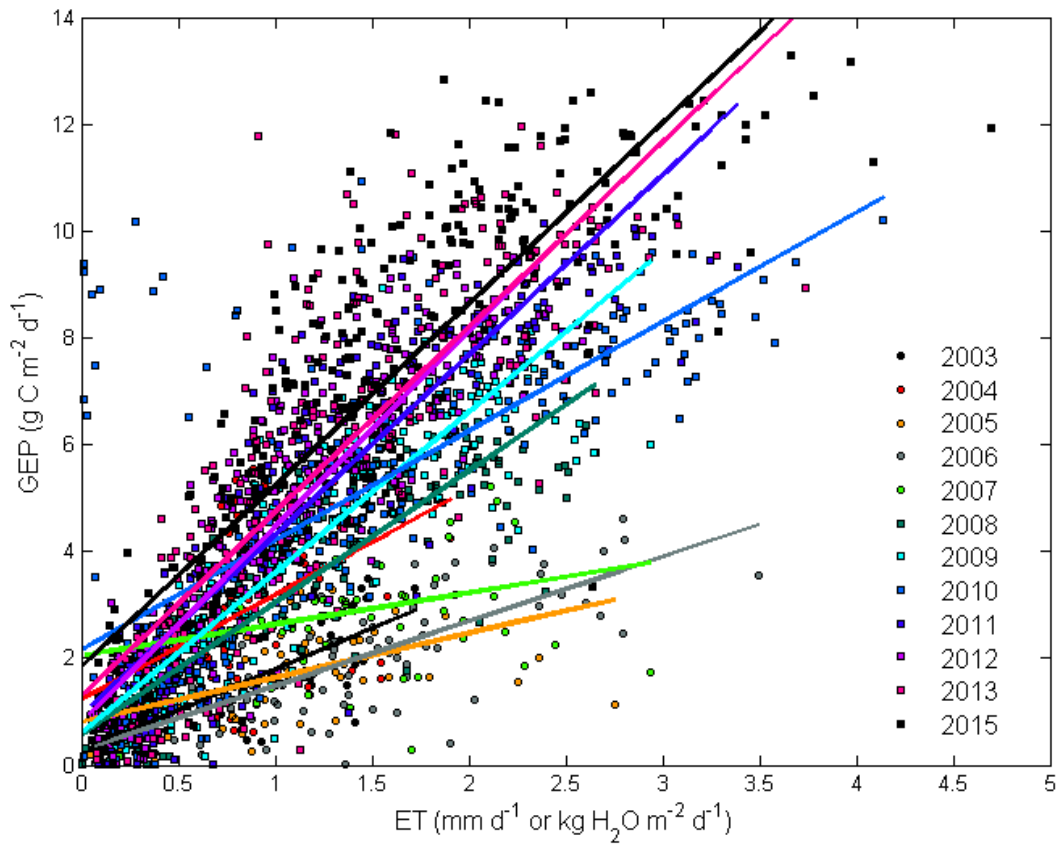


**Figure 14.** Daily water use efficiency (WUE), which is represented by the slope of C assimilated (GEP) and water lost (ET). From 2003 to 2007, 0.29 to 0.61 g of C was sequestered for every kg of water transpired. From 2008 to 2015, 1.36 to 3.95 g of C was sequestered for every kg of water transpired.

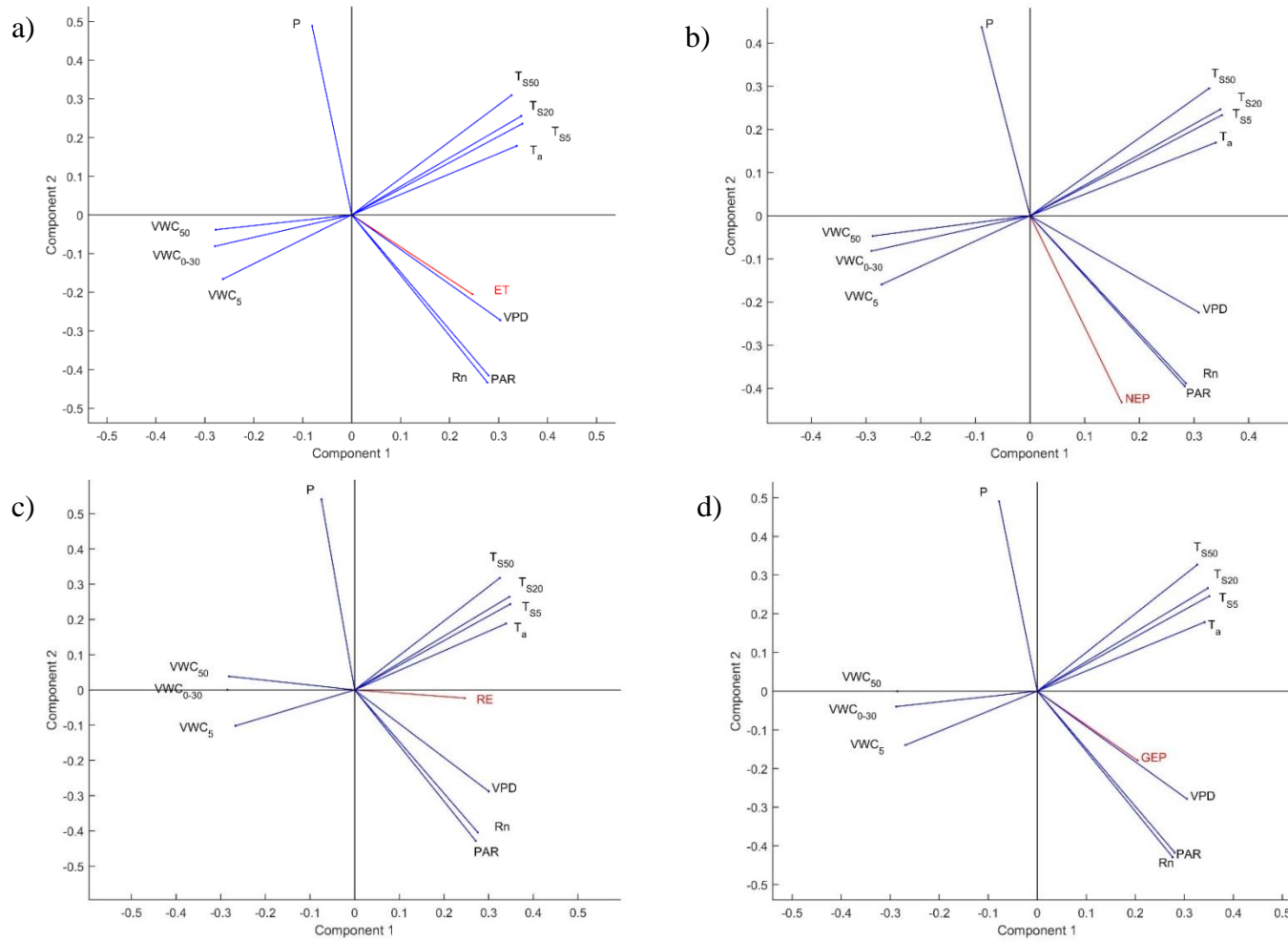


**Figure 15.** Variables factor maps from principal component analysis illustrating the correlation of control variables and their correlation with (a) ET, (b) NEP, (c) RE, and (d) GEP.

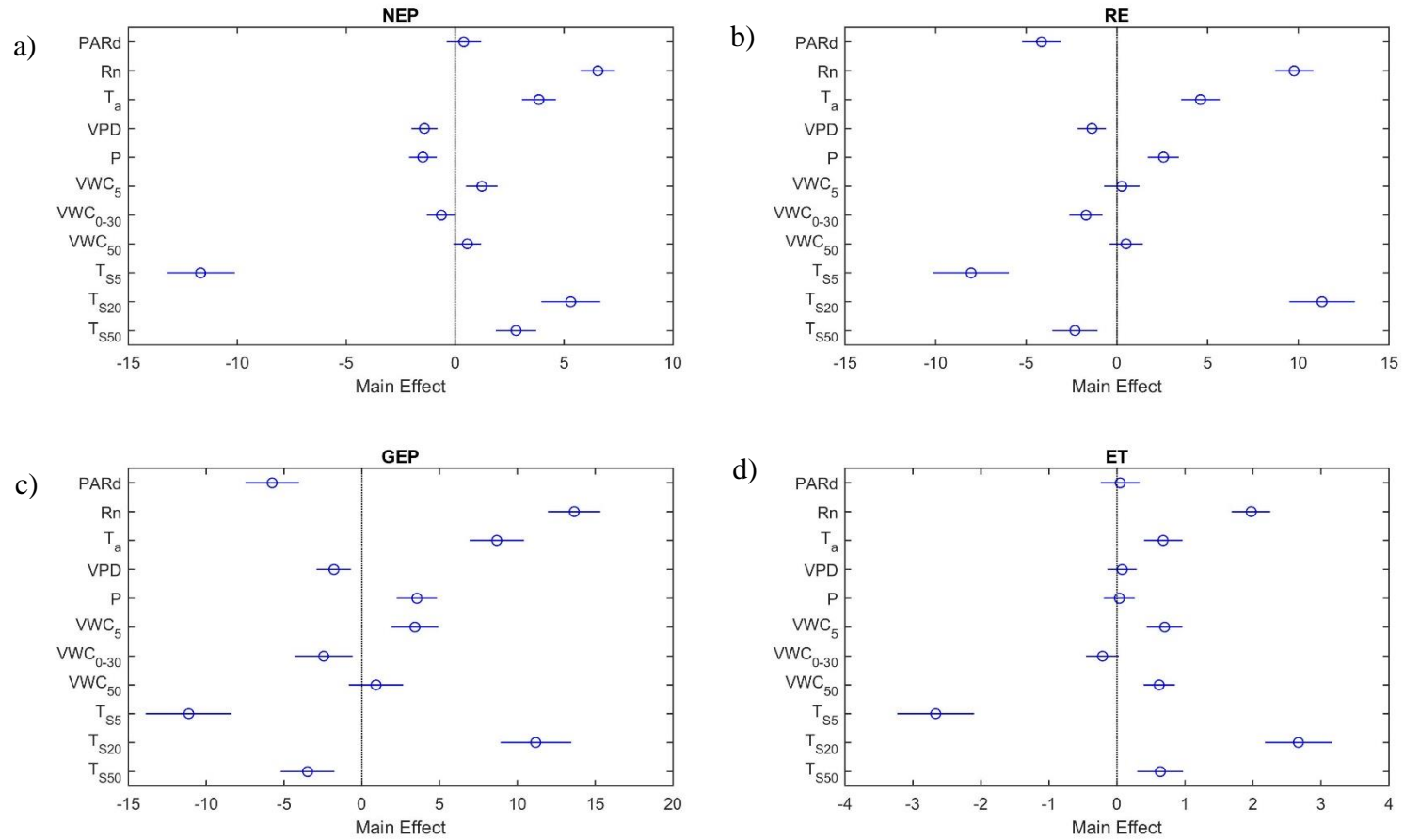


**Figure 16.** Main effect plots of linear regression analyses on the dependent (a) NEP, (b) RE, (c) GEP, and (d) ET variable.

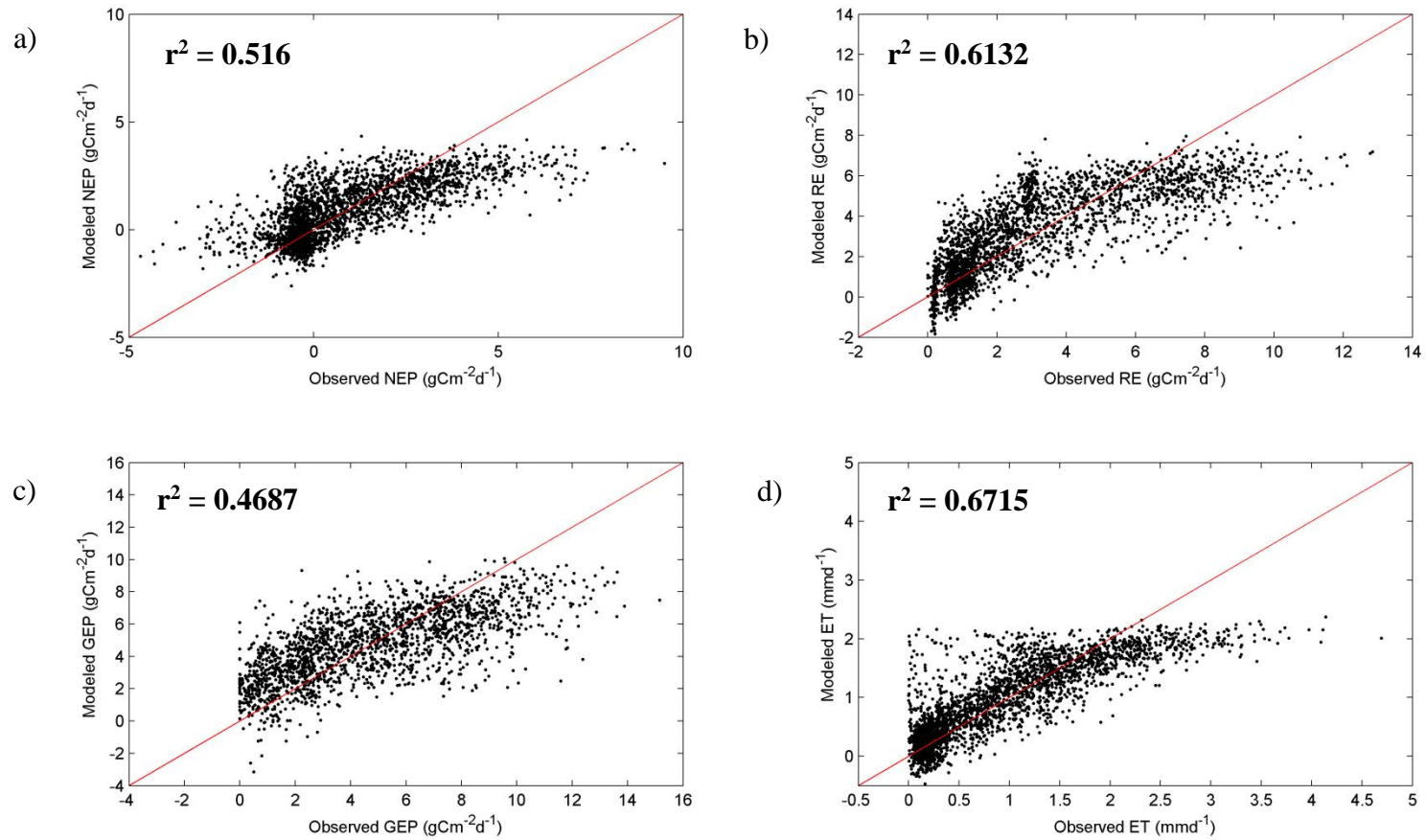


**Figure 17.** Observed versus modeled plots for (a) NEP, (b) RE, (c) GEP, and (d) ET fluxes.

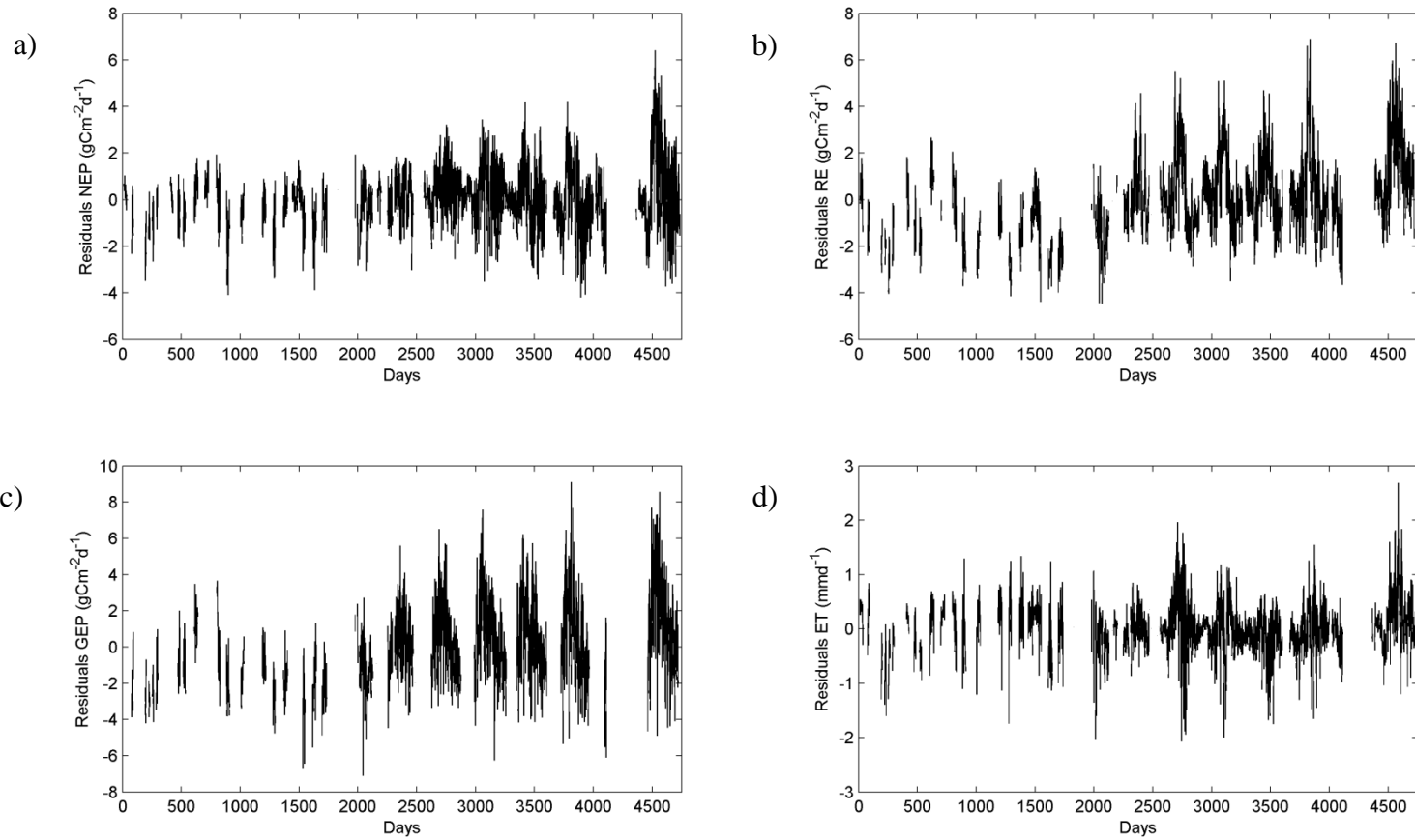


**Figure 18.** Residual plots of (a) NEP, (b) RE, (c) GEP, and (d) ET models.

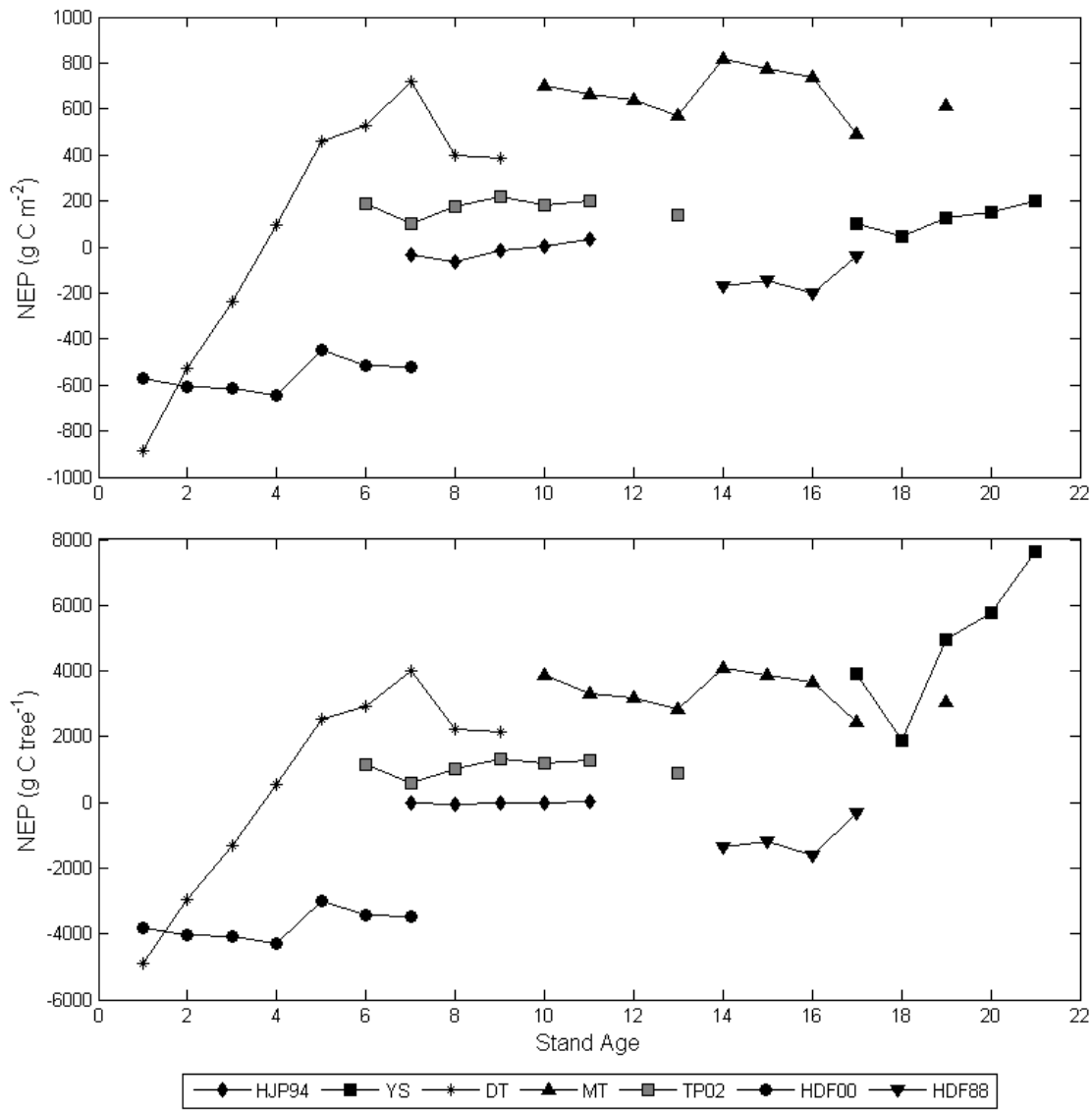


**Figure 19.** a) Comparison of NEP in young stands across North America. HJP94 – boreal jack pine; YS – temperate ponderosa pine; MT – sub-tropical slash pine; DT- sub-tropical slash pine; TP02 – temperate white pine; HDF00 – coastal temperate Douglas-fir; HDF88 – coastal temperate Douglas-fir. b) NEP standardized with tree density (tree m<sup>-2</sup>). See **Supplementary Table 1** for further details.

**SUPPLEMENTARY TABLES****Supplementary Table 1.** Summary table of young flux sites located across North America.

| Site                  | Climate                 | Species        | Stand Establishment  | Year | Age | NEP (g C m <sup>-2</sup> ) | Density (tree m <sup>-2</sup> ) | NEP per tree | Site reference     |
|-----------------------|-------------------------|----------------|--|------|-----|----------------------------|---------------------------------|--------------|--------------------|
| Saskatchewan (HJP94)  | Boreal                  | Jack pine      | Clearcut in 1975, natural regeneration                                     | 2001 | 7   | -32                        | 1.25                            | -26          | Zha et al 2009     |
|                       |                         |                |  | 2002 | 8   | -67                        | 1.25                            | -54          | Zha et al 2009     |
|                       |                         |                |  | 2003 | 9   | -16                        | 1.25                            | -13          | Zha et al 2009     |
|                       |                         |                |  | 2004 | 10  | 4                          | 1.25                            | 3            | Zha et al 2009     |
|                       |                         |                |  | 2005 | 11  | 34                         | 1.25                            | 27           | Zha et al 2009     |
| Metolius, Oregon (YS) | Mediterranean Temperate | Ponderosa pine | Clearcut, stripped of debris, tilled, planted in 1987                      | 2004 | 17  | 102                        | 0.026                           | 3923         | Vickers et al 2011 |
|                       |                         |                |  | 2005 | 18  | 49                         | 0.026                           | 1885         | Vickers et al 2011 |
|                       |                         |                |  | 2006 | 19  | 129                        | 0.026                           | 4962         | Vickers et al 2011 |
|                       |                         |                |  | 2007 | 20  | 150                        | 0.026                           | 5769         | Vickers et al 2011 |
|                       |                         |                |  | 2008 | 21  | 199                        | 0.026                           | 7654         | Vickers et al 2011 |
| Florida (MT)          | Sub-tropical            | Slash pine     | Stem-only clearcut, bedded, herbicide, planted in 1999, fertilized in 2002 | 1999 | 1   | -885                       | 0.18                            | -4917        | Bracho et al 2012  |
|                       |                         |                |  | 2000 | 2   | -528                       | 0.18                            | -2933        | Bracho et al 2012  |
|                       |                         |                |  | 2001 | 3   | -237                       | 0.18                            | -1317        | Bracho et al 2012  |
|                       |                         |                |  | 2002 | 4   | 97                         | 0.18                            | 539          | Bracho et al 2012  |
|                       |                         |                |  | 2003 | 5   | 458                        | 0.18                            | 2544         | Bracho et al 2012  |
|                       |                         |                |  | 2004 | 6   | 527                        | 0.18                            | 2928         | Bracho et al 2012  |
|                       |                         |                |  | 2005 | 7   | 718                        | 0.18                            | 3989         | Bracho et al 2012  |
|                       |                         |                |  | 2006 | 8   | 400                        | 0.18                            | 2222         | Bracho et al 2012  |
| Florida (DT)          | Sub-tropical            | Slash pine     | Clearcut, planted in 1989, fertilized in 1993 and 2001                     | 1999 | 10  | 700                        | 0.18                            | 3889         | Bracho et al 2012  |
|                       |                         |                |  | 2000 | 11  | 663                        | 0.2                             | 3315         | Bracho et al 2012  |
|                       |                         |                |  | 2001 | 12  | 640                        | 0.2                             | 3200         | Bracho et al 2012  |
|                       |                         |                |  | 2002 | 13  | 569                        | 0.2                             | 2845         | Bracho et al 2012  |
|                       |                         |                |  | 2003 | 14  | 818                        | 0.2                             | 4090         | Bracho et al 2012  |

|                        |                      |             |   |      |    |      |        |       |                                |
|------------------------|----------------------|-------------|---|------|----|------|--------|-------|--------------------------------|
|                        |                      |             |   | 2004 | 15 | 775  | 0.2    | 3875  | Bracho et al 2012              |
|                        |                      |             |   | 2005 | 16 | 735  | 0.2    | 3675  | Bracho et al 2012              |
|                        |                      |             |   | 2006 | 17 | 491  | 0.2    | 2455  | Bracho et al 2012              |
|                        |                      |             |   | 2008 | 19 | 613  | 0.2    | 3065  | Bracho et al 2012              |
| Turkey Point<br>(TP02) | Temperate            | White pine  | Afforestation on fallow agricultural land in 2002 | 2008 | 6  | 191  | 0.1683 | 1135  | This paper                     |
|                        |                      |             |   | 2009 | 7  | 100  | 0.1683 | 594   | This paper                     |
|                        |                      |             |   | 2010 | 8  | 173  | 0.1683 | 1028  | This paper                     |
|                        |                      |             |   | 2011 | 9  | 221  | 0.1683 | 1313  | This paper                     |
|                        |                      |             |   | 2012 | 10 | 184  | 0.1567 | 1174  | This paper                     |
|                        |                      |             |   | 2013 | 11 | 198  | 0.1567 | 1264  | This paper                     |
|                        |                      |             |   | 2014 | 12 | n/a  | n/a    | n/a   |                                |
| BC<br>(HDF00)          | Coastal<br>Temperate | Douglas-fir | Clearcut, pile burn, planted in 2000              | 2001 | 1  | -571 | 0.15   | -3807 | Schwalm et al 2007             |
|                        |                      |             |   | 2002 | 2  | -606 | 0.15   | -4040 | Schwalm et al 2007             |
|                        |                      |             |   | 2003 | 3  | -614 | 0.15   | -4093 | Schwalm et al 2007             |
|                        |                      |             |   | 2004 | 4  | -642 | 0.15   | -4280 | Schwalm et al 2007             |
|                        |                      |             |   | 2005 | 5  | -450 | 0.15   | -3000 | Schwalm et al 2007             |
|                        |                      |             |   | 2006 | 6  | -515 | 0.15   | -3433 | Krishnan et al 2009            |
|                        |                      |             |   | 2007 | 7  | -522 | 0.15   | -3480 | modelled;<br>Jassal et al 2010 |
| BC<br>(HDF88)          | Coastal<br>Temperate | Douglas-fir | Clearcut, slash fire, planted in 1988             | 2002 | 14 | -168 | 0.124  | -1355 | Schwalm et al 2007             |
|                        |                      |             |   | 2003 | 15 | -147 | 0.124  | -1185 | Schwalm et al 2007             |
|                        |                      |             |   | 2004 | 16 | -199 | 0.124  | -1605 | Schwalm et al 2007             |
|                        |                      |             |   | 2005 | 17 | -39  | 0.124  | -315  | Schwalm et al 2007             |